Molecular and functional characterization of SlSPL-CNR in tomato fruit ripening and cell death

Tongfei Lai[1*], Xiaohong Wang[1*], Bishun Ye[1*], Mingfei Jin[2,3*], Weiwei Chen[1], Ying Wang[1], Yingying Zhou[1], Andrew M Blanks[4], Mei Gu[5], Pengcheng Zhang[1], Xinlian Zhang[6], Chunyang Li[3], Huizhong Wang[1], Yule Liu[7], Philippe Gallusci[8], Mahmut Tör[9] and Yiguo Hong[1,3,9]

[1]Research Centre for Plant RNA Signaling and Zhejiang Provincial Key Laboratory for Genetic Improvement and Quality Control of Medicinal Plants, College of Life and Environmental Sciences, Hangzhou Normal University, Hangzhou 310036, China

[2]School of Life Sciences, East China Normal University, Shanghai 200241, China

[3]Warwick-Hangzhou Joint RNA Signaling Laboratory, School of Life Sciences, University of Warwick, Coventry CV4 7AL, UK

[4]Cell and Developmental Biology, Division of Biomedical Sciences, Warwick Medical School, University of Warwick, Coventry CV2 2DX, UK

[5]The Gurdon Institute, University of Cambridge, Cambridge CB2 1QN, UK

[6]Department of Family Medicine and Public Health, Division of Biostatistics & Bioinformatics, University of California San Diego, La Jolla, CA 92093, USA

[7]MOE Key Laboratory of Bioinformatics, Centre for Plant Biology, School of Life Sciences, Tsinghua University, Beijing 10084, China

[8]Laboratory of Grape Ecophysiology and Functional Biology, Bordeaux University, INRA, Bordeaux Science Agro, 33882, Villenave d'Ornon, France

[9]Worcester-Hangzhou Joint Molecular Plant Health Laboratory, School of Science and the Environment, University of Worcester, Worcester, WR2 6AJ, UK

[*]These authors contributed equally to this work.

Correspondence: Yiguo Hong, Tel: +86 571 2886 6065;

Email: yiguo.hong@hznu.edu.cn; yiguo.hong@warwick.ac.uk; y.hong@worc.ac.uk

Co-authors:

1) Tongfei Lai: laitongfei@163.com
2) Xiaohong Wang: wangxiaohong0512@sina.cn
3) Bishun Ye: yebishun@hotmail.com
4) Mingfei Jin; mfjin@bio.ecnu.edu.cn
5) Weiwei Chen: 15858223807@163.com
6) Ying Wang: hswangying@sina.cn
7) Yingying Zhou: zhouyingying1992@163.com
8) Andrew Blank: Andrew.blanks@warwick.ac.uk
9) Mei Gu: mei.gu@gurdon.cam.ac.uk
10) Pengcheng Zhang: zpc604@126.com
11) Xinlian Zhang: xizhang@ucsd.edu
12) Chunyang Li: chunyang70@gmail.com
13) Huizhong Wang: whz62@163.com
14) Yule Liu: yuleliu@mail.tsinghua.edu.cn
15) Philippe Gallusci: philippe.gallusci@inra.fr
16) Mahmut Tor: m.tor@worc.ac.uk
17) Yiguo Hong: yiguo.hong@hznu.edu.cn; yiguo.hong@warwick.ac.uk; y.hong@worc.ac.uk

Highlight

We show for the first time that SlSPL-CNR consists of a distinct monopartite NLS, binds to zinc and interacts with SlSnRK1 to affect cell death and tomato fruit ripening.

Abstract

SlSPL-CNR, an SBP-box transcription factor (TF) gene residing at the epimutant *Colourless non-ripening* (*Cnr*) locus, is involved in tomato ripening. This epimutant provides a unique model to investigate the (epi)genetic basis of fruit ripening. Here we report that SlSPL-CNR is a nucleus-localized protein with a distinct monopartite nuclear localization signal (NLS). It consists of four consecutive residues '$_{30}$KRKR$_{33}$' at the N-terminal of the protein. Mutation of the NLS abolishes SlSPL-CNR to localize into nucleus. SlSPL-CNR comprises two zinc-finger motifs (ZFMs) within the C-terminal SBP-box domain. Both ZFMs contribute to zinc-binding activity. SlSPL-CNR can induce cell death in tomato and tobacco. Induction of cell death by SlSPL-CNR is dependent on its nuclear localization. However, the two ZFMs have differential impacts on SlSPL-CNR to induce severe necrosis or mild necrotic ringspot. NLS and ZFM mutants cannot complement *Cnr* fruits to ripen. SlSPL-CNR interacts with SlSnRK1. Virus-induced *SlSnRK1* silencing leads to reduction in expression of ripening-related genes and inhibits ripening in tomato. We conclude that SlSPL-CNR is a multifunctional protein that consists of a distinct monopartite NLS, binds to zinc and interacts with SlSnRK1 to affect cell death and tomato fruit ripening.

Keywords: SlSPL-CNR, cell death, *Colourless non-ripening*, nuclear localization signal, zinc-finger motif, SlSnRK1, tomato (*Solanum lycopersicum*) fruit ripening

Abbreviations: *Cnr*, *Colourless non-ripening*; CoIP, co-immunoprecipitation; GFP, green fluorescent protein; NLS, nuclear localization signal; PVX, *Potato virus X*; Sl, *Solanum lycopersicum* (because of the proliferation of genus-species initials used in literature, we have changed and used *Sl* for *Solanum lycopersicum* in this report); *SlCMT2*, *CHROMOMETHYLASE 2*; *SlDML2, DEMETER-like DNA demethylase 2*; *SlDRM7*, *DOMAINS REARRANGED METHYLTRANSFERASE 7*; *SlMET1*, *METHYLTRANSFERASE 1*; SNF1, SUCROSE NONFERMENTING1; SPL, SQUAMOSA Promoter Binding Protein-like; SlSnRK1, SUCROSE NONFERMENTING1-RELATED PROTEIN KINASE1; TF, transcription factors; VIGC, virus-induced gene complementation; VIGS, virus-induced gene silencing; ZFM, zinc-finger motif; Y2H, Yeast-two-hybrid

Introduction

Cnr is a naturally occurring epimutant in tomato. *Cnr* plants undergo normal growth and development, but fruits cannot ripen and remain colourless. The texture of *Cnr* tomato alters due to a loss of cell-to-cell adhesion in fruit tissues (Eriksson *et al*., 2004). Mapping and positional cloning reveal that the *Cnr* locus harbours an SBP-box gene *CNR* (*LeSPL-CNR*, redesigned as *SlSPL-CNR*) belonging to the SPL gene family of TFs (Manning *et al.*, 2006; Kong *et al*., 2013; Chen et al., 2018). This mutant results from a spontaneous epimutation that causes hypermethylation in the 286bp DNA region of the promoter, approximately 2.4kb upstream of the *SlSPL-CNR* gene coding sequence. *SlSPL-CNR* is developmentally regulated, being mainly expressed in ripening fruits (Manning *et al.*, 2006; Salinas *et al*., 2010), with its expression fine-tuned by *SlymiR157* (*SlmiR157*) to affect fruit ripening (Chen *et al*., 2015a). *Cnr* consists of a hypermethylated epigenome (Zhong *et al*., 2013; Chen *et al*., 2015b), likely due to lack of the expression of *SlDML2* (Liu *et al*., 2015). *SlCMT2*, *SlCMT3*, *SlDRM7* and *SlMET1*, that are key genes in the RNA-directed DNA methylation and methylation maintenance pathways, are required to maintain the *Cnr* epiallele. Inhibition of these genes by VIGS results in ripening reversion in *Cnr* fruits (Chen *et al*., 2015b). Moreover, VIGS of *SlSPL-CNR* leads wild-type tomato (*Solanum lycopersicum* cv Ailsa Craig, AC) to phenocopy the physical, physiological, biochemical and molecular characteristics of *Cnr* fruits (Lai *et al*., 2015).

The *SPL* gene family consists of a group of genes encoding the SBP-box TFs that are unique to plants (Cardon *et al.*, 1999; Zhang *et al*., 2015). SBP-box genes were previously identified in *Antirrhinum majus* and their protein products bind to promoter of the floral meristem identity gene *SQUAMOSA* (Huijser *et al*., 1992; Klein *et al.*, 1996). Subsequently many SBP-box genes have been identified in at least 66 organisms from green algae to flowering plants (Cardon *et al*., 1999; Zhang *et al*., 2015). In tomato, 15 members of the SBP-box gene family have been reported, although most of them are not functionally characterised. Of the SBP-box genes identified to date, *SlSPL-CNR* is closely related to the tomato *SlySBP3* (*SlSBP3*), potato *StSBP3* and *Arabidopsis AtSPL3* genes (Salinas *et al.*, 2012). In plants, SBP-box genes are involved in different growth and development processes such as microsporogenesis and megasporogenesis (Unte *et al.*, 2003), kernel development (Wang *et al.*, 2005), male inflorescence size (Wu *et al*., 2016), male fertility (Xing *et al*., 2010; Xing *et al.*, 2013), plant architecture (Stone *et al.*, 2005), floral transition (Cardon *et al.*, 1997), lateral primordia initiation (Chuck *et al*., 2014), leaf development (Yanaguchi *et al*., 2009; Hou *et al*., 2017), bract development and meristem boundaries (Chuck *et al*., 2010; Preston *et al*., 2010), shoot maturation (Schwarz *et al*., 2008; Shikata *et al*., 2009), ovary and fruit development (Manning *et al*., 2006; Ferreira e Silva *et al*., 2014, Chen *et al*., 2015), as well as ear development and yields (Wu *et al*., 2016; Zhang *et al*., 2014; Wang and Zhang, 2017; Zhang *et al*., 2017). SBP-box TFs are diverse in their

primary protein structures but share a highly-conserved DNA-binding domain of approximate 80 amino-acid (aa) residues. Moreover, the *Arabidopsis* SlSPL-CNR orthologs AtSPL4 and AtSPL7 possess a ZFM (Yamasaki *et al*., 2004) and within the SBP-domain there is a bipartite NLS (Birkenbihl *et al*., 2005). It is also established that the SPL-family TFs such as *A. majus* AmSBP1 and AmSBP2 (Klein *et al*., 1996), AtSPL3 (Cardon *et al*., 1997), AtSPL4, AtSPL7 (Yamasaki *et al*., 2004) and AtSPL8 (Birkenbihl *et al*., 2005), and the single-cell algae *Chlamydomonas* CRR1 (Birkenbihl *et al.*, 2005) bind *in vitro* to the *A. majus SQUAMOSA* and the orthologous *Arabidopsis AP1* promoters.

On the other hand, *SnRK* represents a family of genes encoding SNF1-RELATED PROTEIN KINASES that act as a global regulator of carbon metabolism. In plants the *SnRK* family has been grouped into three sub-families, namely *SnRK1*, *SnRK2* and *SnRK3* (Coello *et al*., 2011). Similar to SBP-box TF genes, *SnRKs* play essential roles in various physiological processes such as leaf senescence (Kim *et al*., 2017), early kernel development (Bledsoe *et al*., 2017), pollen hydration (Liu *et al*., 2016) and development (Zhang *et al*., 2001), cellular energy homeostasis and cell proliferation (Guerinier *et al*., 2013), biotic and abiotic stress (Cho *et al*., 2012; Lin *et al*., 2014; Perochon *et al*., 2015;), cell death and hypersensitive response (Szczesny *et al*., 2010; Avila *et al*., 2013), herbivory tolerance (Schwachtie *et al*., 2006), seed germination and seedling growth (Lu et al., 2007), and crop yield (Lawlor *et al*., 2014). *SnRK1* has been found to be involved in anthocyanin accumulation in apple (Liu *et al*., 2017) and tomato fruit development (Wang *et al*., 2012). More recently, it has been reported that *SnRK2* negatively influences fruit development and ripening in strawberry (Han *et al*., 2015).

In this article, we report on molecular and functional dissection of SlSPL-CNR. Using PCR-based site-directed mutagenesis and a PVX-based transient gene expression system, we reveal that SlSPL-CNR is localized to nucleus through a distinct monopartite NLS and binds to zinc. NLS is required for SlSPL-CNR, but ZFMs may contribute, to trigger plant cell death. SlSPL-CNR requires both NLS and ZFMs to complement ripening in *Cnr* fruits. Using a yeast-two-hybrid screening and CoIP assay, we identified SlSnRK1 as a SlSPL-CNR interacting protein. VIGS of *SlSnRK1* affects expression of a spectrum of ripening-related genes and inhibits ripening in tomato. These results shed light on how SlSPL-CNR acts in tomato fruit ripening. Moreover, our findings also demonstrate that SlSPL-CNR is a multi-functional protein capable of triggering cell death in plants.

Materials and Methods

Plant materials and growth

Wild-type tomato *S. lycopersicum* cv. Ailsa Craig (AC) and *Nicotiana benthamiana* plants were grown in insect-free growth rooms or greenhouses at 25ºC under 16 h light and 8 h dark cycle with a humidity of 60-80%.

Construct

Virus transient vectors to express mutant SlSPL-CNR:GFP fusion proteins were generated as previously described (van Wezel *et al*., 2002). Briefly, mutant SlSPL-CNR coding sequences (Fig. S1; Table S1) were either amplified by standard PCR or overlapping PCR using primers listed in Table S2, and cloned into the PVX/GFP vector to produce PVX/SlSPL-CNR mutant:GFPs (Fig. S2; Fig. S3; Table S2). PVX/SlSPL-CNR:GFP was generated previously (Manning *et al*., 2006). To express free SlSPL-CNR protein, the wild-type *SlSPL-CNR* gene was amplified with PP298 (5'-CCTCACAtcGATGGAAACTAACAAATGGGAAGGGA-3', *Cla* I underlined) and the 3'-end primer (5'-GATGCTcggcCgTCAGCCCAAATTTTCTCCATGAGAG-3', *Eag* I underlined), and cloned into the *Cla* I/*Eag* I sites of the PVX vector (van Wezel *et al*., 2002) to generate PVX/GFP. A 500bp fragment of the *SlSnRK1* gene was amplified by PCR using a cDNA library prepared from the tomato fruit pericarp and cloned to the PVX vector to produce PVX/SlSnRK1 (Data S1). All constructs were verified by DNA sequencing.

Virus transient gene expression and VIGC

Virus transient gene expression was carried out in repeated experiments as previously described (Qin *et al*., 2017). In each experiment, three to six young AC or *N. benthamiana* plants were mock-inoculated or inoculated with recombinant PVX RNAs produced by *in vitro* transcription. VIGC in *Cnr* fruits were performed as previously described (Zhou *et al*., 2012).

Epifluorescence and confocal microscopy

Virus inoculated AC or *N. benthamiana* were routinely examined under long-wave length ultraviolet light (Upland UVP Model B 100AP) to check transient GFP expression and systemic spread of the recombinant viruses. Photographs were taken with a Zeiss Axiophot microscope with filters (excitation at 450 to 490 nm and long-pass emission at 520 nm or excitation at 546 nm and long-pass emission at 590nm) through a Nikon Coolpix 995 digital camera (Li *et al*., 2011). Confocal imaging of the leaves was taken under a Zeiss LSM 710 three-channel microscope with an excitation light of 405 nm, and the emission was captured at 454 to 581nm.

Zinc-affinity pull-down and western blot

Young leaf tissues were collected at 14 days post inoculation, ground in liquid nitrogen and resuspended in extraction buffer (EB; 50mM Tris-HCl [pH 8.0], 1mM phenylmethylsulfonyl fluoride) containing 0, 100 or 400mM NaCl. Insoluble debris were discarded after centrifugation, and supernatants were collected. Zinc-affinity pull-down assays were performed as described (van Wezel *et al*., 2003). Briefly, an equal amount of wild-type or SlSPL-CNR mutant:GFP fusion protein in either 0, 100, or 400 mM NaCl was incubated with a 50-µl aliquot of zinc chelate affinity resins (iminodiacetic acid Sepharose 6B; Sigma) pre-equilibrated with the EB containing either 0 100, or 400mM NaCl, as appropriate. Resins were then washed three times with the same buffer, resuspended in 100-µl gel loading buffer, and boiled for 3 min before loading samples onto a sodium dodecyl sulfate–15% polyacrylamide gel. After electrophoresis, proteins were immobilized on nitrocellulose membranes and immune-detected by use of a SlSPL-CNR or GFP antibody (van Wezel and Hong, 2004).

Y2H screening

Matchmaker Gold Yeast Two-Hybrid System (PT4084-1, Clontech, USA) was performed following the manufacturer's guidance with minor modifications. Briefly, the SlSPL-CNR coding region was PCR amplified using a pair of primers (Y2H_SlSPL-CNR-F: 5'-GAGTCGGAATTCATGGAAACTAACAAATGGGAAGGG-3' and Y2H_SlSPL-CNR-R: 5'-TCGACAGGATCCTCAGCCCAAATTTTCTCCATGAGAG-3'), and cloned into the *EcoR* I/*BamH* I sites of the pGBKT7 vector to generate the bait construct pGBKT7/SlSPL-CNR (Fig. S4; Fig. S5). The integrity of this construct was confirmed by sequencing. For construction of a tomato cDNA library, total RNA was extracted from the pericarp tissues of AC fruits at the breaker stage using an RNAeasy Plant Mini Kit (Qiagen, Germany). Then, oligo dT-primed cDNAs were generated using Make Your Own "Mate & Plate" Library System (PT4085, Clontech, USA-1). Amplification of SMART (Switching Mechanism at 5' end of RNA Transcript) cDNAs by Long Distance PCR was performed using the Advantage 2 Polymerase Mix, and one set of products was size-selected using CHROMA SPIN+TE-400 columns following the protocol of the Clontech's SMART technology. Finally, a sequence homologous to the prey vector pGADT7-Rec was added to a pool of ds cDNAs. The purified SMART ds cDNA, pGADT7-Rec AD Cloning Vector (*Sma*I-linearized) and pGBKT7/SlSPL-CNR were co-transformed into yeast strain AH109 using the Yeastmaker Yeast Transformation System 2 (PT1172-1, Clontech, USA). An aliquot of suspensions of the transformation mixture was spread evenly onto 150 mm plates with SD/-Trp, SD/-Leu/-Trp or SD/-Ade/-His/-Leu/-Trp medium. After incubation at 30 °C for 3-5 days, positive colonies were identified and prey plasmids were extracted by a TIANprep Yeast Plasmid

DNA Kit (Tiangen, China). Inserted cDNA in the pGADT7-Rec vectors were identified by PCR amplification using the T7-primer (5'-TAATACGACTCACTATAGGGC-3') and the AD-primer (AGATGGTGCACGATGCACAG), then sequenced and analysed using an online blast programme (http://blast.ncbi.nlm.nih.gov). Yeast β-galactosidase assay was performed following the manufacture's Yeast Protocols Handbook (Clontech Laboratories, Inc). Student's ***t***-tests were carried out against the negative controls (http://www.physics.csbsju.edu/stats/t-test.html).

To investigate whether the intact SlSnRK1 protein would interact with SlSPL-CNR in yeast, the full-length coding sequence for SlSnRK1 was amplified using the tomato cDNA library as template and a specific set of primers, and cloned into the pGBKT7 and pGADT7 vectors (Fig. S6; Table S4). An extra pGADT7/SlSPL-CNR was also constructed (Fig. S6; Table S4). Y2H for testing SlSnRK1/SlSPL-CNR interaction was performed as described above.

Agroinflitration and Co-IP assay

We constructed pCAMBIA1300/35S-eGFP, pCAMBIA1300/35S-FLAG, pCAMBIA1300/35S-SlSPL-CNR:eGFP and pCAMBIA1300/35S-SlSnRK1:FLAG in the binary pCAMBIA1300 vector (Yu et al., 2018) in order to express free GFP, 3×FLAG, GFP-tagged SlSPL-CNR and 3xFLAG-tagged SlSnRK1 proteins in plants (Fig. S7a; Table S4). These binary gene expression constructs were respectively transformed into *Agrobacterium tumefaciens* GV3101. Two young leaves per *N. benthamiana* plant at the six-leaf stage were infiltrated or co-infiltrated with 1 OD600 agrobacterium harboring different gene expression vectors in repeated experiments as described (Chen et al., 2018). Agro-infiltrated leaf tissues were collected at 3 days post-infiltration (dpi) for further analysis. For analysis of protein expression, total proteins were extracted from *N. benthamiana* leaves (1 g leaf tissues for each sample) using Plant Protein Extraction Kit (CWBIO, www.cwbiotech.com). Protein gel separation and western blot were performed as described above using either antiGFP (Abcam) or antiFLAG antibody (Sigma-Aldrich). CoIP assay was performed using ANTI-FLAG® M2 Magnetic Beads (Sigma-Aldrich). Briefly, total proteins were extracted from *N. benthamiana* leaves (1 g leaf tissues for each sample) in ice-cold buffer (50 mM Tris HCl, pH 7.4, with 150 mM NaCl, 1 mM EDTA, and 1% TRITON X-100). Protein extracts were then incubated with ANTI-FLAG® M2 Magnetic Beads for 12 hr at 4˚C. The precipitations were washed four times with ice-cold immunoprecipitation buffer (50 mM Tris HCl, 150 mM NaCl, pH 7.4) at 4˚C and were analyzed by immunoblot using anti-GFP antibody (Abcam).

VIGS

PVX-based VIGS of *SlSnRK1* expression was performed in AC fruits at various developmental stages on different trusses on the same plants, and on different plants in repeated experiments as

described (Manning *et al*., 2006). In each experiment, pedicels of 30-40 fruits at 5–20 days post anthesis were mock-injected with Tris-EDTA buffer or injected with PVX/SlSnRK1 transcripts. Tomato plants were grown and maintained in growth rooms at 25ºC with supplementary lighting to give a 16-h photoperiod. Fruits were daily examined and photographed with a Nikon Coolpix 995 digital camera.

RT-PCR and qRT-PCR

Total RNA was extracted from *N. benthamiana* leaf tissues or AC pericarp tissues using the RNAeasy Plant Mini Kit (Qiagen). First-strand cDNA was synthesized using equal amounts of total RNA and a FastQuant RT Kit with gDNA Eraser (Tiangen). RT-PCR was performed as previously described (Li *et al*., 2011). Real-time PCR was performed using a CFX96 Real-Time system (Bio-Rad) with the UltraSYBR Mixture (CoWin Bioscience) and gene specific primers (Table S2; Data S1). 18S rRNA was used as an internal control, and at least three biological duplicates and four technical duplicates per biological duplicate were used for each of repeated experiments. The relative expression level was calculated by the Equation $2^{-\Delta\Delta Ct}$ as described (Livak and Schmittgen, 2001; Qin *et a*l., 2012). To analyse gene expression in VIGSed fruits, we dissected the green non-ripe and red ripening sectors and extract total RNAs from each sector. These RNAs were used in qRT-PCR assays along with three different sets of primers (Data S1) in order to examine how VIGS affected the level of *SlSnRK1* mRNA transcripts. The relative expression level in Green or Red sector of VIGSed fruits was further normalized against the level of *SlSnRK1* mRNA in AC fruits at Breaker+5 days (B+5). RT-qPCR data between ripe and non-ripe sectors were analysed by Student's ***t***-test (http://www.physics.csbsju.edu/stats/t-test.html). The statistical significance threshold was $P \leq 0.05$.

DNA methylation assay

The whole genome bisulfite sequencing data were previously generated in our laboratory (Chen *et al*., 2015b) or available online (Zhong *et al*., 2013). Characterization of DNA methylation profiles was performed as previously described (Chen et al., 2015b).

Results

SlSPL-CNR is a nucleus-localized protein and could trigger cell death in tomato

We used PVX/SlSPL-CNR:GFP (Fig. 1) to express the SlSPL-CNR (15kD) and GFP (27kD) fusion protein in *S. lycopersicum* AC plants, and found that green fluorescence was predominantly confined within the nuclei of tomato leaf cells (Fig. 1A,B). In contrast, we observed fluorescence of free GFP

throughout the cytoplasm in cells of tomato leaf tissues infected with PVX/GFP (Fig. 1C). Viral expression of SlSPL-CNR:GFP fusion protein (42kD) and free GFP were detected. PVX infection of AC leaf tissues was further evidenced by immuno-detection of viral coat protein (CP; Fig. 1D). These data demonstrate that the PVX-based transient gene expression system was effective to express SlSPL-CNR:GFP in tomato cells, and that SlSPL-CNR is a nucleus-localized protein. We also observed that PVX/GFP induced chlorotic lesions, typical local symptoms associated with PVX infection (Fig. 1E), whilst virally expressed SlSPL-CNR:GFP elicited cell death and produced severe necrotic lesions on the inoculated AC leaves (Fig. 1F). However, we did not observe cell death in AC fruits which were injected by PVX/SlSPL-CNR:GFP (Manning et al., 2006), likely due to that fusion of GFP might have some negative influence on SlSPL-CNR activity. However, AC fruits treated with PVX/SlSPL-CNR (Fig. 1G) which is expected to express free SlSPL-CNR protein with full functionality developed necrotic cell death (Fig. 1H-J), whilst control AC fruits treated with PVX/GFP remained normal (Fig. 1K).

SlSPL-CNR comprises a distinct monopartite $_{30}$KRKR$_{33}$ NLS

SlSPL-CNR consists of 136aa residues. Similar to other SPB-box TFs, SlSPL-CNR consists of a lysine/arginine (K/R)-rich region $_{109}$KRSCRRRLAGHNERRRK$_{125}$ at its C-terminal. We designated residues $_{109}$KR$_{110}$, $_{113}$RRR$_{115}$ and $_{122}$RRRK$_{125}$ as Domain I, II and III, respectively (Fig. S1). Domain I and Domain III within this region represent a bipartite NLS for several SBP-box TFs (Birkenbihl *et al.*, 2005). To test whether SlSPL-CNR has a similar bipartite NLS, we mutated $_{109}$KR$_{110}$ and $_{122}$RRRK$_{125}$ by substituting the six K/R residues with alanine (A) for virally expressing SlSPL-CNR13:GFP in *N. benthamiana* (Fig. S2). Compared to the negative control (mock inoculation; Fig. 2A), SlSPL-CNR13:GFP was found to localize in cell nucleus, similar to wild-type SlSPL-CNR:GFP fusion protein (Fig. 2B; Table S1).

We then produced PVX constructs to express SlSPL-CNR1:GFP, SlSPL-CNR2:GFP, SlSPL-CNR3:GFP, SlSPL-CNR12:GFP, SlSPL-CNR23:GFP and SlSPL-CNR123:GFP mutant proteins, of which, each of the individual domains (I, II or III) or combinations was replaced with alanine (Fig. S2). Similar to SlSPL-CNR:GFP (Fig. 2B), the single- or double-domain mutated proteins were found to be all cell nucleus-localized (Table S1). The triple-domain mutant protein SlSPL-CNR123:GFP was also predominantly restricted to cell nucleus (Fig. 2C; Table S1). These data indicate that the bipartite NLS shown previously for several SBP-box TFs (Birkenbihl *et al.*, 2005) and the three-consecutive arginine ($_{103}$RRR$_{105}$) residues do not contribute to a functional NLS that determines the nuclear localization of SlSPL-CNR.

This unexpected finding stimulated further examinations of the SlSPL-CNR protein sequence, which revealed two extra basic amino acid-rich domains $_{30}$KRKR$_{33}$ and $_{68}$HRRHK$_{72}$ (dubbed IV and V, respectively; Fig. S1). We then constructed extra 25 viral vectors to express SlSPL-CNR:GFP fusion proteins in which the five basic amino acid-domains were mutated in every possible permutation in order to identify a functional NLS for SlSPL-CNR (Fig. S2). Outcomes of these experiments are summarised in Table S1 and representatives of confocal microscopic images are shown in Fig. 2.

We found that SlSPL-CNR mutants, whichever maintained Domain IV, retained the functionality to translocate the GFP fusion protein to cell nucleus (Table S1). For instance, as SlSPL-CNR:GFP (Fig. 2C), green fluorescence of SlSPL-CNR1235:GFP, in which all K/R residues in Domains I, II, III and V were substituted with A, was predominantly present in cell nucleus (Fig. 2D). On the other hand, SlSPL-CNR derivatives, as long as their Domain IV was mutated, were no longer nuclear-localized (Table S1). Indeed, the single Domain IV-mutated SlSPL-CNR4:GFP failed to localize to nucleus and its GFP fluorescence was present in cytoplasm (Fig. 2E). A similar cytoplasmic appearance of GFP fluorescence was observed for SlSPL-CNR12345:GFP, a quint-mutant protein in which the five basic amino acids-rich domains were all mutated (Fig. 2F). Taken together, these results demonstrate that $_{30}$KRKR$_{33}$ (Domain IV) at the N-terminus represents a distinct monopartite NLS that determines the nuclear localization of SlSPL-CNR in plant cells.

Requirement of NLS for SlSPL-CNR to induce cell death

Expression of the wild-type SlSPL-CNR protein triggered severe necrosis and cell death in tomato leaf tissues. We then investigated how plants responded to the NLS-mutated SlSPL-CNRs (Fig. 3). SlSPL-CNR:GFP or 31 SlSPL-CNR mutant-GFP fusion proteins (Fig. S2) were respectively expressed and a typical necrotic or chlorotic lesion is shown (Fig. 3A-D). Extensive necrosis was found in the lesions resulted from PVX/SlSPL-CNR:GFP infection with many broken chloroplasts observed in dying and dead cells (Fig. 3A,C). Nevertheless, GFP green fluorescence of SlSPL-CNR:GFP was observed predominantly in nuclei of cells around the periphery of the necrotic lesion (Fig. 3A,C). In contrast, healthy cells with intact chloroplasts were found in the lamina of the chlorotic lesion associated with PVX/SlSPL-CNR4:GFP infection. Consistent with this, SlSPL-CNR4:GFP was no longer nucleus-localized and the GFP fluorescence was observed in cytoplasm (Fig 3B,D). SlSPL-CNR mutant proteins that had lost the functional NLS ($_{30}$KRKR$_{33}$) lost the capability to induce cell death, whilst these nucleus-localized mutant proteins maintained their activity to trigger cell death (Table S1).

This finding was supported by the analysis of accumulation of the recombinant PVX RNAs (Fig. 3E), viral CP and SlSPL-CNR:GFP fusion proteins (Fig. 3F). No viral RNA, CP or SlSPL-CNR protein

was detected in mock-inoculated plants. However, specific recombinant *PVX-GFP* or *PVX-CNR-GFP* RNAs were detected in virus-infected leaf tissues (Fig. 3E). Consistently, viral CP was detected in all virus-infected plants. However, wild-type or mutant SlSPL-CNR:GFP fusion proteins were not detected in mock-inoculated or PVX/GFP infected plants, but readily detectable in plants in which SlSPL-CNR:GFP, SlSPL-CNR123:GFP, SlSPL-CNR1235:GFP, SlSPL-CNR12345:GFP or SlSPL-CNR4:GFP was expressed (Fig. 3F).

SlSPL-CNR binds to zinc and the zinc-binding activity contributes to SlSPL-CNR mediated induction of cell death

The SlSPL-CNR protein is predicted to possess two putative ZFMs, named Zn1 and Zn2, within the conserved SBP-domain (Fig. S1). To test whether Zn1 and Zn2 are required for SlSPL-CNR to bind to zinc, we expressed SlSPL-CNR:GFP (wild-type), Zn1- or Zn2-mutated protein SlSPL-CNRmZn1:GFP or SlSPL-CNRmZn2:GFP, or Zn1/Zn2 double-mutant protein SlSPL-CNRmZn12:GFP (Fig. 4; Fig. S3; Table S2). Viral expression of these proteins was evident by the occurrence of the GFP fluorescence in *N. benthamiana* (Fig. 4A-D). SlSPL-CNRmZn1:GFP acted like SlSPL-CNR:GFP to induce severe necrotic cell death (Fig. 4A-1,B-1). However both SlSPL-CNRmZn1:GFP and SlSPL-CNRmZn12:GFP were only able to produce mild necrotic ringspots (Fig. 4C-1,D-1).

Through zinc-affinity pull-down assays, we found that SlSPL-CNR:GFP and the Zn1 mutant protein bound sufficiently to zinc under no NaCl conditions. The wild-type protein remained bound to zinc at 100 or 400mM NaCl. However the zinc-binding ability of SlSPL-CNRZn1:GFP reduced at 100mM NaCl, and no binding was found in the high salt (400mM NaCl; Fig. 4E, left and right panels). Strikingly, both the Zn2 and Zn1/Zn2 single or double-mutants almost completely lost their zinc-binding ability. Only a trace amount of Zn2 and Zn1/Zn2 mutant proteins were detected in the no-salt buffer (Fig. 4E, right panel). We also observed slight degradation of SlSPL-CNR:GFP, SlSPL-CNRmZn1:GFP, SlSPL-CNRmZn2:GFP or SlSPL-CNRmZn12:GFP, evidenced by detection of a band of the similar size of free GFP (Fig. 4E, top right panel). Taken together, our findings demonstrate that SlSPL-CNR is a zinc-binding protein and the Zn2 motif contributes limitedly to the induction of plant cell death.

Requirement of functional NLS and ZFMs for SlSPL-CNR to complement Cnr mutant

To assess whether SlSPL-CNR requires the monopartite NLS and the two ZFMs to influence fruit ripening, we exploited a VIGC assay (Zhou *et al*., 2012) to express wild-type, NLS- or ZFM-mutated *Sl*SPL-CNR in *Cnr* fruits (Fig. 5). Similar to our previous analysis (Kong *et al.*, 2013), approximately 15% of *Cnr* fruits that were injected with PVX/SlSPL-CNR:GFP turned orange-red (Fig. 5A), suggesting

that the wild-type SlSPL-CNR expressed from the recombinant virus could at least partially complement and lead the *Cnr* mutant fruits to ripen to a certain degree. However all *Cnr* fruits that were injected with PVX/SlSPL-CNR4:GFP, PVX/SlSPL-CNRmZn1:GFP or PVX/SlSPL-CNRZn2 remained non-ripe, showing the typical 'colourless non-ripening' phenotypes (Fig. 5A). Presence of the respective recombinant viruses and expression of the wild-type or mutant SlSPL-CNR mRNA in the *Cnr* fruits were readily detected either by western blot using the PVX CP antibody or RT-PCR (Fig. 5B,C). These findings demonstrate that functional NLS and ZFMs are required for SlSPL-CNR to carry out its proper activity to induce ripening reversion in the *Cnr* fruits.

SlSnRK1 interacts with SlSPL-CNR

To understand how SlSPL-CNR affects fruit ripening in tomato, we used SlSPL-CNR as bait (Fig. S4A) to screen a tomato fruit prey cDNA library (Fig. S4B) in Y2H system to identify SlSPL-CNR-interacting proteins. We obtained 80 positive yeast colonies for DNA sequencing (Fig. S4C-E) and produced 47 good sequences. In total, 20 candidate genes were identified through blasting these sequences against the NCBI database (https://www.ncbi.nlm.nih.gov/). Three of the 47 original sequences were matched to *SlSnRK1* (Data S1; Bradford *et al.*, 2003; Avila *et al.*, 2012). The longest codes the C-terminal 183aa portion of SlSnRK1 (Fig. S5A) and their interactions with SlSPL-CNR were further verified (Fig S5B,C). Moreover, we cloned the full-length SlSnRK1 coding sequence in-frame fused to the GAL4 activating and DNA-binding domain, as well as SlSPL-CNR in-frame fused to the GAL4 DNA binding domain (Fig. S6). In two different configurations, the full-length SlSnRK1 protein was found to be able to interact with SlSPL-CNR (Fig. 6A,B).

Using CoIP assay, we further examined if SlSPL-CNR interacts with SlSnRK1 in plants (Fig S7A-J; Fig. 7). Both SlSPL-CNR:eGFP (42kD) and SlSnRK1:FLAG (64kD) fusion proteins were readily detectable by either anti-GFP or anti-FLAG antibody (Fig. S7K,L; Fig. 7A,B). SlSPL-CNR:eGFP was shown to be co-precipitated with SlSnRK1:FLAG (Fig. 7C). Moreover, expression of SlSPL-CNR:eGFP triggered cell death in agro-infiltrated tissues (Fig. S7F,I,J), consistent with virus-transient expression assays. Collectively, our results clearly demonstrate that SlSPL-CNR can interact with SlSnRK1 in both yeast and plant cells.

Silencing of SlSnRK1 inhibits tomato ripening

To investigate the biological relevance of the SlSPL-CNR/SlSnRK1 interaction in tomato, we first analysed *SlSnRK1* expression profiles in AC and *Cnr* fruits at various ripening stages and in different tissues (Fig. S8). The qRT-PCR data indicate that expression of *SlSnRK1* underwent dynamic changes during fruit development and ripening (Fig. S8A). Such oscillation in the *SlSnRK1* transcript levels

from 27 (30) to 42 (45) DPA was particularly consistent with the RNA transcriptome analysis (Fig. S8B; original RPKM (Reads Per Kilobase of transcript per Million mapped reads) were from http://www.epigenome.cuhk.edu.hk/encode.html). Interestingly, the *SlSnRK1* mRNA level was slightly higher at most stages in *Cnr* than AC fruits. This is in contrast to that *SlSnRK1* was expressed more in AC stems, leaves and flowers than in the equivalent *Cnr* tissues, whilst no difference was found in AC and *Cnr* roots (Fig. S8C).

We then used VIGS to examine how *SlSnRK1* would affect fruit ripening (Fig. 8). To achieve this, pedicels of a total of 60-80 AC fruits at 5–20 days post anthesis were mock-injected with Tris-EDTA buffer or injected with the empty VIGS vector PVX or PVX/SlSnRK1 (Fig. 8A; Data S1). In all mock- or PVX-injected AC fruits, fruits developed and ripened normally (Fig. 8B,C). However, approximately 20% of AC fruits injected with PVX/SlSnRK1 showed delayed or non-ripening phenotypes (Fig. 8D,E), consistent with VIGS-mediated suppression of *SlSnRK1* gene expression in the non-ripe sectors of these fruits (Fig. 8F; Fig. S9). It would be worthwhile mentioning that 20% of injected fruits showed phenotypes are typical in our tomato VIGS experiments (Manning et al., 2006; Lin et al., 2008, Chen et al., 2015b; Lai et al., 2015).

To confirm the impact of *SlSnRK1* VIGS on tomato ripening, we analysed expression of a range of ripening-related genes in the green non-ripe and red-ripe sectors of the *SlSnRK1*-silenced AC fruits. These genes include key ripening TF genes, ethylene biosynthesis and responsive genes (Fig. S10), and genes coding enzymes for biosynthesis of lycopene, abscisic acid (ABA), carotenoids and flavonoids (Fig. S11; Fig. S12; Fig. S13). Consistent with the non-ripe phenotypes, expression levels of most of these genes were reduced in the non-ripe sectors compared to the red-ripe sectors in the *SlSnRK1*-silencing fruits. For instance, expression of *TDR4*, *RIN*, *NOR*, *NR* and *SlSPL-CNR* was found to be markedly reduced in the non-ripe sectors. We also found a decrease in the expression level of ethylene biosynthesis and responsive genes such as *ACO1*, *ACO3*, *ACO4*, *ACS2*, *ACS3* and *EBF2* (Fig. S10). Similarly, expression levels of lycopene, carotenoids and flavonoids biosynthesis genes including *PSY1, PSY2*, *PDS*, *ZDS*, *Z-ISO* or *ANS* were reduced. The genes coding the key enzyme NCED for ABA biosynthesis was also decreased in the *SlSnRK1*-silenced non-ripe fruits (Fig. S11).

Differential methylation in the SlSnRK1 promoter

Compared to AC, *Cnr* fruit possesses a hypermethylated epigenome revealed by previously whole genome bisulfite sequencing studies in our and other laboratories (Zhong *et al*., 2013; Chen *et al*., 2015b). Using the latest tomato genome and epigenome databases, we analysed the DNA methylation profiles for *SlSnRK1*, particularly in the 5,000-bp promoter sequences prior to the coding

region (Fig. S14). Two differentially methylated regions (DRMs) were identified in the *SlSnRK1* promoter. These DMRs were found to be highly methylated in *Cnr* compared to AC at 42-days post anthesis. Interestingly, silencing of *SlCMT3*, which led to ripening reversion in *Cnr* fruits (Chen *et al*., 2015b), reduced the DNA methylation level in both DMRs in the VIGS fruits compared to non-VIGS *Cnr* controls (Fig. S14A,B). We interpret these results to mean that expression of *SlSnRK1*, similar to *SlSPL-CNR*, could be influenced by some epigenetic mechanism to affect fruit ripening in tomato.

Comparative whole genome bisulfide sequencing analyses also imply that the *SlSnRK1* gene expression may be epigenetically affected. Expression of *SlSnRK1* occurred in fruits as well as other tissues in both AC and *Cnr*. This gene seems to be affected by *Cnr* (Fig. S8), further suggesting that *SlSnRK1* may be influenced by an epigenetic mechanism and that SlSnRK1 may operate on SlSPL-CNR to affect fruit development and ripening. Interestingly, the levels of *SlSnRK1* mRNA in both AC and *Cnr* fruits are not that much different. It may be possible that in AC, the amount of SlSnRK1 protein translated from the limited amount of *SlSnRK1* transcripts might be sufficient to affect SlSPL-CNR function. On the other hand, higher levels of DNA methylation in cis regulatory regions generally inhibit gene transcription. Nonetheless, single-base resolution profiling of whole tomato genome methylation along with transcriptome analysis have revealed many exceptions where the opposite effects occur (Zhong et al., 2013). It could be that higher methylation in the cis differentially methylated sequences may block a repressor(s) to interact with the *SlSnRK1* promoter, resulting in a high level of *SlSnRK1* transcription in *Cnr*. However, any impact of SlSnRK1 on SlSPL-CNR in *Cnr* would be minimal due to the transcriptional blockage of *SlSPL-CNR* expression. Thus, these results may also imply that *SlSnRK1* may impose an epistatic influence on *SlSPL-CNR*, presumably via a physical interaction between the two protein products, and subsequent phosphorylation of SlSPL-CNR by the kinase activity of SlSnRK1 (Fig. 9).

Discussion

SlSPL-CNR has been shown to be involved in tomato fruit ripening. Suppression of *SlSPL-CNR* by an epimutation is responsible for the pleiotropic phenotypes in *Cnr* fruits (Thompson *et al*., 1999; Eriksson *et al*., 2004; Manning *et al*., 2006). The *Cnr* epimutant also provides an important tool for investigating the (epi)genetic basis of tomato development and fruit ripening (Zhong *et al*., 2013; Chen *et al*., 2015; Liu *et al*., 2015). However, biochemical dissection of the SlSPL-CNR protein and the molecular mechanism about how this small TF affects tomato fruit ripening remain unknown. In this article, we report on the following discoveries:

(1) SlSPL-CNR has a distinct NLS and localised in the nucleus (Fig. 1; Fig. 2). This unique NLS consists of '$_{30}$KRKR$_{33}$' at the N-terminal of SlSPL-CNR. Mutation of the monopartite NLS completely abolishes SlSPL-CNR to localize into nucleus despite the putative bipartite NLS at the C-terminal remains intact (Fig. 2; Fig. S1), differing from the bipartite NLS reported for other SBP-box TFs such as AtSPL3 and AtSPL8 (Birkenbihl *et al.*, 2005). Intriguingly, the monopartite NLS is so unique that no such equivalent $_{30}$KRKR$_{33}$ signal sequence has been found in AtSPL3, AtSPL8 and other SBP-box TFs (Birkenbihl *et al.*, 2005).

(2) SlSPL-CNR is a zinc-binding protein that comprises two ZFMs Zn1 and Zn2 within the C-terminal conserved SBP-box domain, and both ZFMs are involved in zinc-binding (Fig. 4E; Fig. S1). However, loss of Zn2 almost completely eliminates the zinc-binding activity of SlSPL-CNR. On the other hand, the Zn1-mutated SlSPL-CNR protein can still bind to zinc, albeit with a lower affinity, than the wild-type protein (Fig. 4E). We observed that the intensity of the GFP fluorescence in plants expressing SlSPL-CNRmZn2:GFP or SlSPL-CNRmZn12:GFP was weaker than that found in plants expressing the wild-type SlSPL-CNR:GFP or SlSPL-CNRmZn1:GFP (Fig. 4A-D). This suggest that the Zn2- and Zn1/Zn2-mutants were less stable than the wild-type and Zn1 mutant SlSPL-CNR proteins in plant cells. Nevertheless, our findings are consistent with previous reports that both ZFMs are important for SBP-box TFs to bind to zinc and DNA in a zinc-dependent manner (Yamasaki *et al*., 2004; Birkenbihl *et al*., 2005).

(3) VIGC reveals that both NLS and ZFMs are functionally required for SlSPL-CNR to affect fruit ripening (Fig. 5), elucidating previously unknown impacts of NLS and ZFMs on SlSPL-CNR in tomato fruit ripening. It should be noted that during our VIGC experiments, we photographically recorded the change of these treated *Cnr* fruits. Partial complementation was well correlated with the viral transient expression of the wild-type *SlSPL-CNR* gene, but not with the any mutated forms of *SlSPL-CNR* although the PVX coat protein could be detected in all these fruits (Fig. 5). From our experience, a change of fruit colour is a valid indication of fruit ripening, as shown in our previous works (Manning et al., 2006, Lin et al., 2008; Zhou et al. 2012; Chen et al., 2015a; 2015b and 2018). In addition to its functionality in fruit ripening, SlSPL-CNR can also induce cell death in tomato and tobacco leaf tissues as well as in tomato fruits (Fig. 1; Fig.3; Fig.4; Fig. S7), indicating SlSPL-CNR is a multifunctional protein. Consistent with this idea, SlSPL-CNR was found to be expressed in leaves, early and late vegetative shoot apices, inflorescences, sepals, petals and carpels although mainly in ripening fruits (Salinas *et al*., 2010). Considering (1) transient expression of SlSPL-CNR via two means (i.e. virus- and aginfiltration-based vectors) caused cell death; (2) NLS was required for SlSPL-CNR to induce cell death; and (3) the two ZFMs were differentially involved in induction of cell death, we believe that activation of cell death is unlikely an artificial act for SlSPL-CNR. Moreover, viral ectopic

expression of TFs does not always trigger cell death. For instance, LeMADS-RIN (SlMADS-RIN) when expressed from the same PVX-based vector caused no cell death, but resulted in virus-induced gene complementation (Zhou et al., 2012). Another example is that viral expression of LeHB1 (SlHB1) initiated no cell death whilst disrupted flower development (Lin et al., 2008). Both SlMADS-RIN and SlHB1 are two important ripening TFs in tomato. In addition, both stress-related genes and *DAD-1* encoding the Defender against cell death-1 were also found to be up-regulated in *Cnr* (Eriksson et al., 2004). Taken together, these different lines of evidence suggest that causing cell death could probably be a genuine function of SlSPL-CNR along with its role in tomato ripening.

(4) In yeast and plant cells, SlSPL-CNR interacts with SlSnRK1 (Fig. 6; Fig.7; Fig. S4-S7). Moreover, the C-terminal 183-aa sequences of SlSnRK1 may have contributed to its interaction with SlSPL-CNR (Fig. S5), although any precise interacting domain(s) needs to be further defined. To our knowledge, this is the first partner protein to be found to interact with SlSPL-CNR.

(5) Suppression of *SlSnRK1* by VIGS inhibits fruit ripening and leads to reduction in the expression level of a wide range of ripening-related genes (Fig. 8; Fig. S9-S13). In these VIGSed AC fruits, only 20-30% reduction was observed in green sectors using the two sets of primers corresponding to the 5'- or middle portion of SlSnRK1. However, detection using a third pair of primers corresponding to the 3' end of *SlSnRK1* showed more than 50% reduction of RNA transcript levels (Fig. 8F). These data indicate that the two sets of primers corresponding to the 5' and middle parts of the gene likely picked up some untranslatable *SlSnRK1* mRNAs. Thus, the amount of *SlSnRK1* RNA detected in green portions might not be distinctively lower. It is also worthwhile noting that the level of *SlSnRK1* mRNA tends to increase around breaker (35-37 DPA) and red-ripe stage (40 DPA) (Fig. S8). These factors may contribute to relatively low gene repression effect, yet a strong phenotype in these VIGSed AC fruits. Nevertheless, detections using all three sets of primers produced a very similar tendency of decreased *SlSnRK1* levels in green sectors when compared to red sectors.

Together, these collective findings suggest that *SlSnRK1* transcription and subsequent post-translational SlSPL-CNR/SlSnRK1 interaction are of biological relevance to tomato fruit ripening (Fig. S14; Fig. 9). Indeed, VIGS experiments revealed that *SlSnRK1* is involved in fruit ripening. Our working model (Fig. 9) suggests that involvement of *SlSnRK1* in fruit ripening might be via the physical protein interaction between the *SlSnRK1* gene product and SlSPL-CNR, and subsequent phosphorylation of SlSPL-CNR by the kinase activity of SlSnRK1. Such phosphorylation of SlSPL-CNR by SlSnRK1 is supposed to occur in cytoplasm. Translocation of phosphorylated SlSPL-CNR from cytoplasm to nucleus is mainly determined by the unique monopartite NLS. However, a potential requirement of phosphorylation of SlSPL-CNR for its transferring to the nucleus is also possible. We

are now trying to design experiments to test if phosphorylation of SlSPL-CNR by SlSnRK1 occurs, and if interfering with this process would interrupt nuclear localization of CNR, cell death and ripening as predicted by our working model.

Interestingly, transgenic over-expression of a heterologous *MhSnRK1* gene isolated from *Malus hupehensis* reported to increase carbon assimilation and nitrogen uptake in tomato. Moreover, fruits expand faster at the early stage of development after anthesis and fruit-set, and reach the breaker/colour-turning point earlier in the *MhSnRK1* transgenic tomato plants compared to non-transgenic controls (Wang *et al*., 2012). These findings suggest that *MhSnRK1* may act as a facilitator for fruit ripening in the transgenic plants, consistent with suppression of fruit ripening by *SlSnRK1* VIGS (this study). However, in strawberry (*Fragaria* X *ananassa*), FaSnRK2 has been found to interact with ABSCISIC ACID INSENSITIVE1, a negative regulator in fruit ripening. RNAi of *FaSnRK2* significantly promotes whilst over-expression of *FaSnRK2* arrests ripening, demonstrating that *FaSnRK2* negatively impacts on fruit ripening in strawberry (Han *et al*., 2015). These observations may suggest complex and different functions of SnRKs in climacteric and non-climacteric fruit ripening. Moreover, *SnRK1* family genes including *SlSnRK1* have been found in response to biotic and abiotic stress, cell death and hypersensitive response in tomato and a wide range of plants (Szczesny *et al*., 2010; Cho *et al*., 2012; Avila *et al*., 2013; Lin *et al*., 2014; Perochon *et a*l., 2015). It is thus possible that the SlSPL-CNR/SlSnRK1 interactions may be also required for induction of necrosis in plants.

Recently, using CRISPR/Cas9 gene editing technique, Gao et al. (2019) produced *Cnr* and *nor* knockout mutants whilst Wang et al. (2019) generated null mutants for *ap2a*, *nor* and *ful1/2* in order to re-evaluate functions of these TFs in tomato development and fruit ripening. Interestingly, the bioengineered *ap2a* null mutants produced delayed ripening fruits as those in RNAi lines (Wang et al., 2019). However, CRSIPR/Cas9 knockout mutants for *Cnr*, *nor* and *ful1*/2 all failed to phenocopy non-ripening as seen in each of the naturally occurring mutants or in RNAi or VIGS fruits (Gao et al., 2019; Wang et al., 2019). Such phenotypic discrepancies raise an intriguing issue about the precise functionality of the four TFs in tomato fruit ripening. Different hypotheses such as dominant-negative protein, gain-of-function, overlapping functions or functional redundancy have been put forward in order to explain how CNR, NOR as well as FUL1/FUL2 act in tomato ripening. On the other hand, genetically engineered knockout mutants of genes essential for development do not often show any obvious phenotype as shown in naturally occurring mutants or in silencing/RNAi-based knockdown lines. This phenomenon is not uncommon and has been well studied in animals, although seldom reported in plants. It could be explained by genetic compensation, more specifically, transcriptional adaptation that has been shown to be triggered by non-sense mutated

mRNA degradation in mice and zebrafish (El-Brolosy et al., 2019; Ma et al., 2019). By analogy, the tomato knockouts vs knockdown/natural mutants may represent rare examples of genetic compensation in plants, reinforcing that TFs such as *SlSPL-CNR*, *NOR* and *FUL1/2* may play essential roles not only in fruit ripening but also in other physiological processes.

Summary

We report that the SlSPL-CNR protein, an SBP-box TF, can affect tomato fruit ripening and cause cell death in tomato and tobacco plants. Considering the enzymatic activities of SlSnRK1 in phosphorylation of proteins, we envisage a working model that may provide a plausible explanation about how SlSPL-CNR functions as a multi-functional protein to activate tomato fruit ripening and to trigger plant cell death (Fig. 9). We propose that SlSPL-CNR might be post-translationally phosphorylated by SlSnRK1 through their direct physical interactions in cytoplasm. Indeed, SlSnRK1 has been shown to have protein phosphorylation activity (Su and Devarenne, 2018) and it can phosphorylate its interacting partner in tomato (Shen et al., 2011). Thus, a phosphorylated SlSPL-CNR protein might be then translocated from cytoplasm to nucleus, which is mainly determined via the unique monopartite NLS. Once located in cell nucleus, SlSPL-CNR might bind to promoters in a zinc-dependent manner to turn on or off expression of target genes associated with cell death and fruit ripening..

Acknowledgments

We are grateful to David Baulcombe for providing the original PVX vector, Simon Santa-Cruz for providing the GFP and PVX coat protein antisera, and Kenneth Manning for providing the SlSPL-CNR antibody. This work was supported by grants from the Ministry of Science & Technology of China (2017YFE0110900 to Y.H.), the Ministry of Agriculture of China (2016ZX08009001-004 to Y.H.); the National Natural Science Foundation of China (31872636 and 31370180 to Y.H.; 31401926 to T.L.); the Zhejiang Provincial Natural Science Foundation of China (LY18C150009 to T.L.); Hangzhou Normal University (9995C5021841101 and PD201108 to Y.H.); the Hangzhou City S&D Bureau (20131028 to Y.H.); the UK Biotechnology and Biological Sciences Research Council (BBS/E/H/00YH0271 to Y.H.); and the UK Royal Society (RG072176 to Y.H.).

References

Avila J, Gregory OG, Su D, Deeter TA, Chen S, Silva-Sanchez C, Xu S, Martin GB, Devarenne TP. 2012. The β-subunit of the SnRK1 complex is phosphorylated by the plant cell death suppressor Adi3. Plant Physiology **159,** 1277-1290.

Birkenbihl RP, Jach G, Saedler H, Huijser P. 2005. Functional dissection of the plant-specific SBP-domain: overlap of the DNA-binding and nuclear localization domains. Journal of Molecular Biology **352,** 585-596.

Bledsoe SW, Henry C, Griffiths CA, Paul MJ, Feil R, Lunn JE, Stitt M, Lagrimini LM. 2017. The role of Tre6P and SnRK1 in maize early kernel development and events leading to stress-induced kernel abortion. BMC Plant Biology **17,** 74.

Bradford KJ, Downie AB, Gee OH, Alvarado V, Yang H, Dahal P. 2003. Abscisic acid and gibberellin differentially regulate expression of genes of the SNF1-related kinase complex in tomato seeds. Plant Physiology **132,** 1560-1576.

Cardon GH, Höhmann S, Nettesheim K, Saedler H, Huijser P. 1997. Functional analysis of the *Arabidopsis thaliana* SBP-box gene SPL3: a novel gene involved in the floral transition. Plant Journal **12,** 367-377.

Cardon GH, Hohmann S, Klein J, Nettesheim K, Saedler H, Huijser P. 1999. Molecular characterization of the *Arabidopsis* SBP-box genes. Gene **237,** 91-104.

Chen W, Kong J, Lai T, *et al.* 2015a. Tuning *LeSPL-CNR* expression by SlymiR157 affects tomato fruit ripening. Scientific Reports **5,** 7852.

Chen W, Kong J, Qin C, *et al.* 2015b. Requirement of *CHROMOMETHYLASE3* for somatic inheritance of the spontaneous tomato epimutation *Colourless non-ripening*. Scientific Reports **5,** 9192.

Chen W, Yu Z, Kong J, *et al.* 2018. Comparative WGBS identifies genes that influence non-ripe phenotype in tomato epimutant Colourless non-ripening. Science China Life Sciences **61,** 244-252.

Chen W, Zhang X, Fan Y, *et al.* 2018. A genetic network for systemic RNA silencing in plants. Plant Physiology **176,** 2700-2719.

Cho YH, Hong JW, Kim EC, Yoo SD. 2012. Regulatory functions of SnRK1 in stress-responsive gene expression and in plant growth and development. Plant Physiology **158,** 1955-1964.

Chuck GS, Brown PJ, Meeley R, Hake S. 2014. Maize SBP-box transcription factors unbranched2 and unbranched3 affect yield traits by regulating the rate of lateral primordia initiation. Proceedings of the National Academy Sciences, USA **111,** 18775-18780.

Chuck G, Whipple C, Jackson D, Hake S. 2010. The maize SBP-box transcription factor encoded by *tasselsheath4* regulates bract development and the establishment of meristem boundaries. Development **137,** 1243-1250.

Coello P, Hey SJ, Halford NG. 2011. The sucrose non-fermenting-1-related (SnRK) family of protein kinases: potential for manipulation to improve stress tolerance and increase yield. Journal of Experimental Botany **62,** 883-893.

El-Brolosy MA, Kontarakis Z, Rossi A, *et al*. 2019. Genetic compensation triggered by mutant mRNA degradation. Nature **568,** 193-197.

Eriksson EM, Bovy A, Manning K, Harrison L, Andrews J, Silva JD, Tucker GA, Seymour GB. 2004. Effect of the *Colorless non-ripening* mutation on cell wall biochemistry and gene expression during tomato fruit development and ripening. Plant Physiology **136,** 4184-4197.

Ferreira e Silva GF, Silva EM, Azevedo Mda S, Guivin MA, Ramiro DA, Figueiredo CR, Carrer H, Peres LE, Nogueira FT. 2014. microRNA156-targeted SPL/SBP box transcription factors regulate tomato ovary and fruit development. Plant Journal **78,** 604-618.

Gao XQ, Liu CZ, Li DD, Zhao TT, Li F, Jia XN, Zhao XY, Zhang XS. 2016. The *Arabidopsis* KINβγ subunit of the SnRK1 complex regulates pollen hydration on the stigma by mediating the level of reactive oxygen species in pollen. PLoS Genetics **12,** e1006228.

Gao Y, Zhu N, Zhu X, *et al*. 2019. Diversity and redundancy of the ripening regulatory networks revealed by the fruitENCODE and the new CRISPR/Cas9 CNR and NOR mutants. Horticultural Research **6**, 39.

Guérinier T, Millan L, Crozet P, *et al*. 2013. Phosphorylation of p27(KIP1) homologs KRP6 and 7 by SNF1-related protein kinase-1 links plant energy homeostasis and cell proliferation. Plant Journal **75,** 515-525.

Han Y, Dang R, Li J, *et al*. 2015. SUCROSE NONFERMENTING1-RELATED PROTEIN KINASE2.6, an ortholog of OPEN STOMATA1, is a negative regulator of strawberry fruit development and ripening. Plant Physiology **167,** 915-930.

Hou H, Yan X, Sha T, Yan Q, Wang X. 2017. The SBP-Box Gene *VpSBP11* from Chinese wild Vitis is involved in floral transition and affects leaf development. International Journal of Molecular Sciences **18,** E1493.

Huijser P, Klein J, Lonnig WE, Meijer H, Saedler H, Sommer H. 1992. Bracteomania, an inflorescence anomaly, is caused by the loss of function of the MADS-box gene *SQUAMOSA* in *Antirrhinum majus*. EMBO Journal **11,** 1239-1249.

Kim GD, Cho YH, Yoo SD. 2017. Regulatory functions of cellular energy sensor SNF1-related kinase1 for leaf senescence delay through *ETHYLENE- INSENSITIVE3* repression. Scientific Reports **7,** 3193.

Klein J, Saedler H, Huijser P. 1996. A new family of DNA-binding proteins includes putative transcriptional regulators of the *Antirrhinum majus* floral meristem identity genes *SAUAMOSA*. Molecular and General Genetics **259,** 7-16.

Kong J, Chen W, Shen J, *et al*. 2013. Virus-induced gene complementation in tomato. Plant Signaling & Behavior **8,** e27142.

Lai T, Wang Y, Zhou T, Mei F, Zhang P, Zhou Y, Shi N, Hong Y. 2015. Virus-induced *LeSPL-CNR* silencing inhibits fruit ripening in tomato. Journal of Agricultural Sciences **7,** 184-194.

Lawlor DW, Paul MJ. 2014. Source/sink interactions underpin crop yield: the case for trehalose 6-phosphate/SnRK1 in improvement of wheat. Frontiers in Plant Sciences **5,** 418.

Li C, Gu M, Shi N, *et al*. 2011. Mobile FT mRNA contributes to the systemic florigen signalling in floral induction. Scientific Reports **1,** 73.

Lin CR, Lee KW, Chen CY, Hong YF, Chen JL, Lu CA, Chen KT, Ho TH, Yu SM. 2014. SnRK1A-interacting negative regulators modulate the nutrient starvation signaling sensor SnRK1 in source-sink communication in cereal seedlings under abiotic stress. Plant Cell **26,** 808-827.

Lin Z, Hong Y, Yin M, Li C, Zhang K, Grierson D. 2008. A tomato HD-Zip homeobox protein, LeHB-1, plays an important role in floral organogenesis and ripening. Plant Journal **55,** 301-310.

Liu R, How-Kit A, Stammitti L, *et al*. 2015. A DEMETER-like DNA demethylase governs tomato fruit ripening. Proceedings of the National Academy Sciences, USA **112,** 10804-10809.

Liu XJ, An XH, Liu X, Hu DG, Wang XF, You CX, Hao YJ. 2017. MdSnRK1.1 interacts with MdJAZ18 to regulate sucrose-induced anthocyanin and proanthocyanidin accumulation in apple. Journal of Experimental Botany **68,** 2977-2990.

Livak KJ, Schmittgen TD. 2001. Analysis of relative gene expression data using real-time quantitative PCR and the 2-DDCT method. Methods **25,** 402–408.

Lu CA, Lin CC, Lee KW, Chen JL, Huang LF, Ho SL, Liu HJ, Hsing YI, Yu SM. 2007. The SnRK1A protein kinase plays a key role in sugar signaling during germination and seedling growth of rice. Plant Cell **19,** 2484-2499.

Ma Z, Zhu P, Shi H, *et al*. 2019. PTC-bearing mRNA elicits a genetic compensation response via Upf3a and COMPASS components. Nature **568,** 259-263.

Manning K, Tor M, Poole M, Hong Y, Thompson AJ, King GJ, Giovannoni JJ, Seymour GB. 2006. A naturally occurring epigenetic mutation in a gene encoding an SBP-box transcription factor inhibits tomato fruit ripening. Nature Genetics **38,** 948-962.

Perochon A, Jianguang J, Kahla A, Arunachalam C, Scofield SR, Bowden S, Wallington E, Doohan FM. 2015. *TaFROG* Encodes a Pooideae Orphan Protein That Interacts with SnRK1 and Enhances Resistance to the Mycotoxigenic Fungus *Fusarium graminearum*. Plant Physiology **169,** 2895-906.

Preston JC, Hileman LC. 2010. *SQUAMOSA*-PROMOTER BINDING PROTEIN 1 initiates flowering in *Antirrhinum majus* through the activation of meristem identity genes. Plant Journal **62,** 704-712.

Qin C, Chen W, Shen J, *et al*. 2017. A Virus-induced assay for functional dissection and analysis of monocot and dicot flowering time genes. Plant Physiology **174,** 875-885.

Qin C, Shi N, Gu M, *et al*. 2012. Involvement of *RDR6* in short-range intercellular RNA silencing in *Nicotiana benthamiana*. Scientific Reports **2,** 467.

Salinas M, Xing S, Hohmann S, Berndtgen R, Huijser P. 2012. Genomic organization, phylogenetic comparison and differential expression of the SBP-box family of transcription factors in tomato. Planta **235,** 1171-1184.

Schwachtje J, Minchin PE, Jahnke S, van Dongen JT, Schittko U, Baldwin IT. 2006. SNF1-related kinases allow plants to tolerate herbivory by allocating carbon to roots. Proceedings of the National Academy Sciences, USA **103,** 12935-12940.

Schwarz S, Grande AV, Bujdoso N, Saedler H, Huijser P. 2008. The microRNA regulated SBP-box genes *SPL9* and *SPL15* control shoot maturation in *Arabidopsis*. Plant Molecular Biology **67,** 183-195.

Shen Q, Liu Z, Song F, Xie Q, Hanley-Bowdoin L, Zhou X. 2011 Tomato SlSnRK1 protein interacts with and phosphorylates βC1, a pathogenesis protein encoded by a geminivirus β-satellite. Plant Physiology **157,** 1394–1406.

Shikata M, Koyama T, Mitsuda N, Ohme-Takagi M. 2009. *Arabidopsis* SBP-box genes *SPL10*, *SPL11* and *SPL2* control morphological change in association with shoot maturation in the reproductive phase. Plant and Cell Physiology **50,** 2133-2145.

Stone JM, Liang X, Nekl ER. Stiers JJ. 2005. *Arabidopsis AtSPL14*, a plant-specific SBP-domain transcription factor, participates in plant development and sensitivity to fumonisin B1. Plant Journal **41,** 744-754.

Szczesny R, Büttner D, Escolar L, Schulze S, Seiferth A, Bonas U. 2010. Suppression of the AvrBs1-specific hypersensitive response by the YopJ effector homolog AvrBsT from *Xanthomonas* depends on a SNF1-related kinase. New Phytologist **187,** 1058-1074.

Su D, Devarenne TP. 2018. In vitro activity characterization of the tomato SnRK1 complex proteins. Biochimica et Biophysica Acta – Proteins and Proteomics **1866,** 857-886.

Thompson AJ, Tor M, Barry CS, Vrebalov J, Orfila C, Jarvis MC, Giovannoni JJ, Grierson D, Seymour GB. 1999. Molecular and genetic Characteization of a novel pleiotropic tomato-ripening mutant. Plant Physiology **120,** 383-389.

Unte US, Sorensen AM, Pesaresi P, Gandikota M, Leister D, Saedler H, Huijser P. 2003. *SPL8*, an SBP-box gene that affects pollen sac development in Arabidopsis. Plant Cell **15,** 1009-1019.

van Wezel R, Dong X, Liu H, Tien P, Stanley J, Hong Y. 2002. Mutation of three cysteine residues in Tomato yellow leaf curl virus-China C2 protein causes dysfunction in pathogenesis and posttranscriptional gene-silencing suppression. Molecular Plant-Microbe Interactions **15,** 203-208.

van Wezel R, Hong Y. 2004. Virus survival of RNA silencing without deploying protein-mediated suppression in *Nicotiana benthamians.* FEBS Letters **562,** 65-70.

van Wezel R, Liu H, Wu Z, Stanley J, Hong Y. 2003. Contribution of the zinc finger to zinc and DNA binding by a suppressor of posttranscriptional gene silencing. Journal of Virology **77,** 696-700.

Wang L, Zhang Q. 2017. Boosting rice yield by fine-tuning SPL gene expression. Trends in Plant Science **22,** 643-645.

Wang R, Tavano ECDR, Lammers M, Martinelli AP, Angenent GC, de Maagd RA. 2019. Re-evaluation of transcription factor function in tomato fruit development and ripening with CRISPR/Cas9-mutagenesis. Scientific Reports **9,** 1696.

Wang X, Peng F, Li M, Yang L, Li G. 2012. Expression of a heterologous SnRK1 in tomato increases carbon assimilation, nitrogen uptake and modifies fruit development. Journal of Plant Physiology **169,** 1173-1182.

Wu X, Li Y, Shi Y, *et al*. 2016. Joint-linkage mapping and GWAS reveal extensive genetic loci that regulate male inflorescence size in maize. Plant Biotechnology Journal **14,** 1551-1562.

Wu Z, Cao Y, Yang R, Qi T, Hang Y, Lin H, Zhou G, Wang ZY, Fu C. 2016. Switchgrass SBP-box transcription factors PvSPL1 and 2 function redundantly to initiate side tillers and affect biomass yield of energy crop. Biotechnology for Biofuels **9,** 101.

Xing S, Salinas M, Garcia-Molina A, Höhmann S, Berndtgen R, Huijser P. 2013. *SPL8* and miR156-targeted SPL genes redundantly regulate Arabidopsis gynoecium differential patterning. Plant Journal **75,** 566-577.

Xing S, Salinas M, Höhmann S, Berndtgen R, Huijser P. 2010. miR156-targeted and nontargeted SBP-box transcription factors act in concert to secure male fertility in *Arabidopsis*. Plant Cell **22,** 3935-3950.

Yamasaki K, Kigawa T, Inoue M, *et al*. 2004. A novel zinc-binding motif revealed by solution structures of DNA-binding domains of *Arabidopsis* SBP-family transcription factors. Journal of Molecular Biology **337,** 49-63.

Yamaguchi A, Wu MF, Yang L, Wu G, Poethig RS, Wagner D. 2009. The microRNA-regulated SBP-Box transcription factor SPL3 is a direct upstream activator of LEAFY, FRUITFULL and APETALA1. Developmental Cell **17,** 268-278.

Yu Z, Chen Q, Chen W, *et al*. 201). Multigene editing via CRISPR/Cas9 guided by a single-sgRNA seed in *Arabidopsis*. Journal of Integrative Plant Biology **60,** 376-381.

Zhang B, Liu X, Zhao G, Mao X, Li A, Jing R. 2014. Molecular characterization and expression analysis of Triticum aestivum squamosa-promoter binding protein-box genes involved in ear development. Journal of Integrative Plant Biology **56,** 571-581.

Zhang B, Xu W, Liu X, Mao X, Li A, Wang J, Chang X, Zhang X, Jing R. 2017. Functional conservation and divergence among homoeologs of *TaSPL20* and *TaSPL21*, two SBP-Box genes governing yield-related traits in hexaploid wheat. Plant Physiology **174,** 1177-1191.

Zhang S-D, Ling L-Z, Yi T-S. 2015. Evolution and divergence of SBP-box genes in land plants. BMC Genomics **16,** 787.

Zhang Y, Shewry PR, Jones H, Barcelo P, Lazzeri PA, Halford NG. 2001. Expression of antisense SnRK1 protein kinase sequence causes abnormal pollen development and male sterility in transgenic barley. Plant Journal **28,** 431-441.

Zhong S, Fei Z, Chen YR, *et al*. 2013. Single-base resolution methylomes of tomato fruit development reveal epigenome modifications associated with ripening. Nature Biotechnology **31,** 154-159.

Zhou T, Zhang H, Lai T, *et al*. 2012. Virus-induced gene complementation reveals a transcription factor network in modulation of tomato fruit ripening. Scientific Reports **2,** 836.

Figure legends

Fig. 1 Expression of SlSPL-CNR induces necrotic cell death. (A) Diagrammatic of viral transient gene expression vector PVX/SlSPL-CNR:GFP. Genome organisation of PVX/GFP and two cloning sites are indicated. RDRP is the viral RNA-dependent RNA polymerase. The triple-gene block encodes three viral movement proteins of 25, 12 and 8kD. GFP was fused in-frame to SlSPL-CNR to express a fusion protein. CP is the viral coat protein. (B) Nuclear localization of SlSPL-CNR:GFP in tomato leaf epidermal cells. (C) Cytoplasmic localization of free GFP protein in tomato leaf epidermal cells. Photographs were taken under an epifluorescence microscope at 7 days post-inoculation (dpi). (D) Western blot detection of SlSPL-CNR:GFP fusion protein. Protein samples were extracted from young tomato leaf tissues at 14dpi. Immuno-detection was performed using either a GFP antibody (upper panel) or a PVX CP antibody (lower panel). (E and F) Induction of necrotic cell death in tomato leaf tissues. Tomato leaves inoculated with PVX/GFP (E) or PVX/SlSPL-CNR (F) developed chlorotic or necrotic lesions, respectively. Photographs were taken at 7dpi. (G-K) Induction of necrotic cell death in tomato AC fruits. AC fruits injected with PVX/SlSPL-CNR (G) developed necrosis at different stages including mature green (H), breaker/colour turning (I) and ripening (J). An AC fruit infected with PVX/GFP (A) ripened and remained healthy (K). All fruits were photographed at 33 days post-injection.

Fig. 2 Characterization of the nuclear localization signal for SlSPL-CNR. (A) Mock-inoculated *N. benthamiana* (*Nb*) leaf cells as a negative control. (B-F) *Nb* leaf cells expressing SlSPL-CNR:GFP (B), SlSPL-CNR123:GFP (C), SlSPL-CNR1235:GFP (D), SlSPL-CNR4:GFP (E) or SlSPL-CNR12345:GFP (F). *Nb* Leaves were taken at 7 days post inoculation and examined under a confocal microscope. Bar=100µm.

Fig. 3 Requirement of a functional NLS for SlSPL-CNR to induce necrotic cell deaths. (A-D) Representative of images of necrotic and chlorotic lesions. Necrotic cell death is associated with the wild-type SlSPL-CNR:GFP protein (A and C). Chlorotic lesions consist of healthy cells expressing the SlSPL-CNR4:GFP protein (B and D). Photographs of lesions/leaf cells were taken at 7-days post inoculation (dpi) under an epifluorescence microscope (A and B) or confocal microscope (C and D). The inlet pictures of a necrotic cell death lesion in (A) and a chlorotic lesion in (B) were photographed under normal light. GFP fluorescence is green and chlorophyll autofluorescence is red. Necrotic dead tissues appear yellow. Bar = 1mm in A and B, Bar = 500nm in C and Dd. Arrows indicate either nuclear or cytoplasmic localization of SlSPL-CNR:GFP (C) or SlSPL-CNR4:GFP (D). (E) RT-PCR detection of recombinant PVX RNA or 18S rRNA as indicated. RNA samples were extracted from young leaf tissues at 14dpi. Sizes and positions of DNA ladders as well as positions of target

genes are indicated. (F) Western blot detection of PVX CP and the wild-type and mutant SlSPL-CNR:GFP fusion proteins. Upper panel: CP antibody, lower panel: SlSPL-CNR antibody. Sizes and positions of protein markers as well as CP and SlSPL-CNR:GFP fusion protein are indicated.

Fig. 4 Involvement of zinc-finger motif in induction of necrotic cell death. (A-D) Impact of mutations in zinc-finger motifs on SlSPL-CNR to trigger severe necrosis. Expression of SlSPL-CNR:GFP (A), SlSPL-CNRmZn1:GFP (B), SlSPL-CNRmZn2:GFP (C) or SlSPL-CNRmZn12:GFP (D) is indicated by the GFP green fluorescence in young leaves. Severe necrosis (A-1 and B-1) and mild necrotic ringspot (C-1 and D-1) are indicated for each of the corresponding fusion proteins. Entire plants were photographed under long-wavelength UV light at 14 days post inoculation (dpi), whilst lesions were photographed under white light at 7dpi. (E) Zinc-affinity pull-down assay. Proteins were detected using either anti SlSPL-CNR or GFP antibody as indicated. The SeeBlue™ Plus2 Pre-stained Protein Standard (Invitrogen) was included in gels. Sizes and positions of protein markers are indicated. SlSPL-CNR:GFP fusion (CNR:GFP, 42kD) and GFP free protein (27kD) as well as NaCl concentration (mM) used in the washing buffer are also indicated.

Fig. 5 Requirement of functional nuclear localization signal and zinc finger motifs in SlSPL-CNR mediated ripening reversion in *Cnr* fruits. (A) Virus-induced gene complementation in the *Cnr* fruits. Representative *Cnr* fruits that were injected with PVX/SlSPL-CNR:GFP (Cnr + CNR:GFP) were ripe. These *Cnr* fruits that were injected with PVX/SlSPL-CNR4:GFP (Cnr + CNR4:GFP), PVX/SlSPL-CNRmZn1:GFP (Cnr + CNRmZn1:GFP) or PVX/SlSPL-CNRmZn2:GFP (Cnr + CNRmZn2:GFP) remained colorless non-ripening. Wild type AC fruits were included as positive controls. Fruits were photographed at 45-days post anthesis. (B and C) Western blot detection of PVX CP and RT-PCR assays of viral transient SlSPL-CNR:GFP mRNA in *Cnr* fruits. Fruits were mock-treated or injected with recombinant PVXs as indicated in (A). Sizes and positions of protein markers and the 1-Kb DNA ladder as well as PVX CP and viral SlSPL-CNR:GFP mRNA are indicated.

Fig. 6 Interactions between SlSPL-CNR and SlSnRK1. (A) Interactions between SlSPL-CNR and SlSnRK1 in two Y2H conformations. P: positive control – yeast strain AH109 carrying both pGBKT7-53 and pGADT7-T. N: negative control – AH109 strain only. Samples 1-7 are indicated. Yeasts were cultured on YPDA agar plates (YPDA), synthetically defined (SD) medium plate without supplement of leucine (Leu) and tryptophan (Trp; SD/-Leu-Trp), or SD without supplement of adenine (Ade), histidine (His), Leu and Trp (SD/-Ade-His-Leu-Trp). Positive interaction between SlSPL-CNR and SlSnRK1 resulted in AH109 growth in SD/-Ade-His-Leu-Trp plates (P; Samples 4 and 5). (B) Quantitative analysis of protein-protein interactions using β-galactosidase activity assay. β-galactosidase assays were performed following Clontech's protocol. 1 unit of β-galactosidase is defined as the amount which hydrolyzes 1 µmol of o-nitrophenyl β-D-galactopyranoside to o-nitrophenol and D-galactose per min

per cell. Samples are indicated as in (A). Three biological duplicates (n=3) for each sample in two separate experiments were used in the β-galactosidase assays (Mean ± S.D). Bars represent standard deviation (S.D.). Student's ***t***-tests were carried out against the negative control (N). P-values are indicated. The statistically significant increases in the β-galactosidase activity in AH109 co-transformed with pGBKT7/SlSPL-CNR + pGADT7/SlSnRK1 or pGBKT7/SlSnRK1 + pGADT7/SlSPL-CNR confirm positive interactions between SlSPL-CNR and SlSnRK1.

Fig. 7 CoIP assays of interaction between SlSPL-CNR and SlSnRK1. (A and B) Detection of SlSPL-CNR:eGFP or SlSnRK1:FLAG in *N. benthamian* (Nb). Total proteins were extracted from Nb leaves at 3 days post-infiltration or co-infiltration with *A. tumefaciens* GV3101/pCAMBIA1300/35S-eGFP (eGFP) and GV3101/pCAMBIA1300/35S-SlSnRK1:FLAG (SlSnRK1:FLAG); GV3101/pCAMBIA1300/35S-FLAG (FLAG) and GV3101/pCAMBIA1300/35S-SlSPL-CNR:eGFP (SlSPL-CNR:eGFP); or GV3101/pCAMBIA1300/35S-SlSnRK1:FLAG and GV3101/pCAMBIA1300/35S-SlSPL-CNR:eGFP. Western blots were probed either with anti-3xFLAG antibody (A, upper panel) or anti-GFP antibody (B, upper panel). Positions for SlSnRK1:FLAG, SlSPL-CNR:eGFP fusion proteins as well as free eGFP are indicated by red arrow. Equal loading of protein samples were illustrated by Coomassie Blue staining gels (lower panel in a and b). (C) Detection of co-immunoprecipitated SlSPL-CNR:eGFP. Total proteins extracted from co-agroinfitrated Nb leaf tissues were absorbed with Anti-FLAG®M2 Magnetic Beads, and analyzed by western blot using Anti-GFP antibody. Co-immunoprecipitation of SlSPL-CNR:eGFP by SlSnRK1:FLAG primarily occurred in leaf tissues co-infiltrated with GV3101/pCAMBIA1300/35S-SlSnRK1:FLAG and GV3101/pCAMBIA1300/35S-SlSPL-CNR:eGFP. The co-immunoprecipitated SlSPL-CNR:eGFP was readily detected by the antiGFP antibody. The positions and sizes of protein marker are indicated.

Fig. 8 Silencing of *SlSnRK1* inhibits tomato fruit ripening. (A) Schematic of the VIGS vector PVX/SlSnRK1. Genome organisation of PVX and the two cloning sites are indicated. RDRP is the viral RNA-dependent RNA polymerase. The triple-gene block encodes three viral movement proteins of 25, 12 and 8kD. CP is the viral coat protein. (B-E) VIGS of *SlSnRK1*. Mock-treated (B) and PVX-injected (C) AC fruits ripened. Fruits injected with PVX/SlSnRK1 developed non-ripe sectors (D and E). Fruits were photographed at 5 days after breaker (45 days post anthesis). Fruits were sectioned in half to show ripe (B and C) or non-ripe (D) pericarps. Three more *SlSnRK1*-silenced AC fruits are shown in (E). (F) qRT-PCR analysis of *SlSnRK1* expression in *SlSnRK1*-silenced AC fruits. Expression of *SlSnRK1* was reduced by VIGS in non-ripe sectors (green bar) compared to the ripe sectors (red bar). qRT-PCRs were performed using three different sets of primers which target to specific amplification of the 5'-, middle (M)- or 3'-end of the *SlSnRK1* gene (Data S1). The relative levels of the *SlSnRK1* transcripts against 18S rRNA differed among the three target RNA sequences, suggesting that VIGS

efficiency as well as the transitivity of VIGS against the three portions of the *SlSnRK1* mRNA may be different. For each fruit we dissected the green non-ripe and red ripening sectors and extract total RNAs from each sectors. These RNAs were used in qRT-PCR assays along with three different sets of primers in order to examine how VIGS affected the level of SlSnRK1 mRNA transcripts. The relative expression level in Green or Red sector of VIGSed fruits was further normalized against the level of SlSnRK1 mRNA in AC fruits at 40 days post anthesis. Student's ***t***-test shows that the expression difference is of statistical significance (P=0.05). qRT-PCRs were performed on at least three different fruits and similar data were obtained for each fruit. Fig. 8F represents the data generated from fruit shown in Fig. 8D, normalized against the fruit in Fig. 8B.

Fig. 9 A working model – Involvement of SlSnRK1 and SlSPL-CNR in cell death and fruit ripening in tomato. Epigenetic control may contribute to an extra layer of regulation of *SlSPL-CNR* and *SlSnRK1* (indicated by a question mark) expression in AC and *Cnr* tomato cell nucleus (Fig, S14; Zhang *et al.*, 2013, Chen *et al.*, 2015). SlSPL-CNR may undergo a post-translational phosphorylation in order to trigger its TF activity in cytoplasm. Such cellular protein modification may be processed by SlSnRK1 through its direct interactions with the SlSPL-CNR protein (shown by a question mark). A phosphorylated SlSPL-CNR protein (designed SlSPL-CNR^{P}, question mark) is then translocated via the unique monopartite NLS from cytoplasm to nucleus. However, phosphorylation per se may or may not be required for nuclear transportation of SlSPL-CNR^{P}. Once located in cell nucleus, SlSPL-CNR^{P} may bind to promoters in a zinc-dependent manner as for other SPB-box TFs to transcriptionally turn on or off expression of specific target genes associated with cell death and fruit ripening, which then leads to phenotypic induction of cell death or/and fruit ripening. Necrotic cell death on the tomato leaf and fruit as well as fruit with non-ripe sectors caused by either transient expression of SlSPL-CNR or virus induced gene silencing are shown. Leaf was photographed at 7 days post-inoculation and fruits at 40 days after anthesis, respectively.

Figure 1

Fig. 1

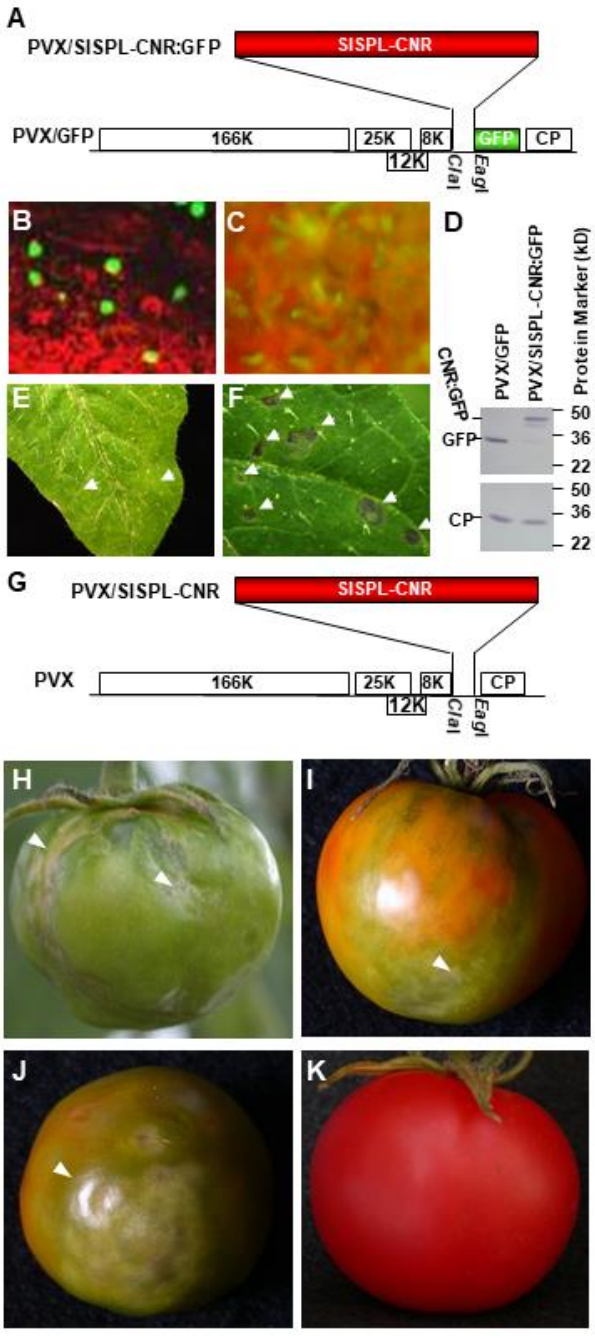

Figure 2

Fig. 2

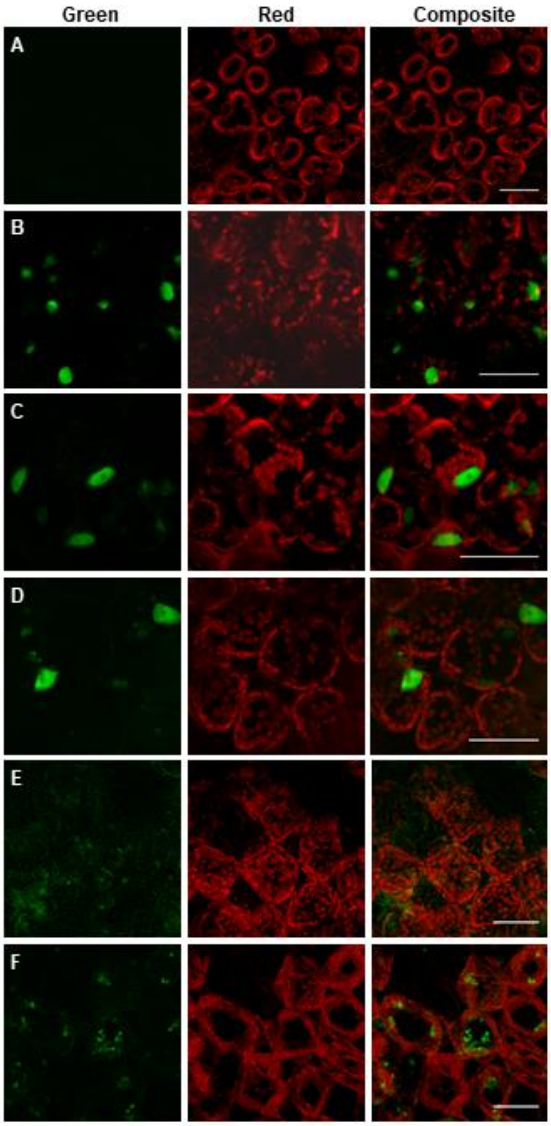

Figure 3

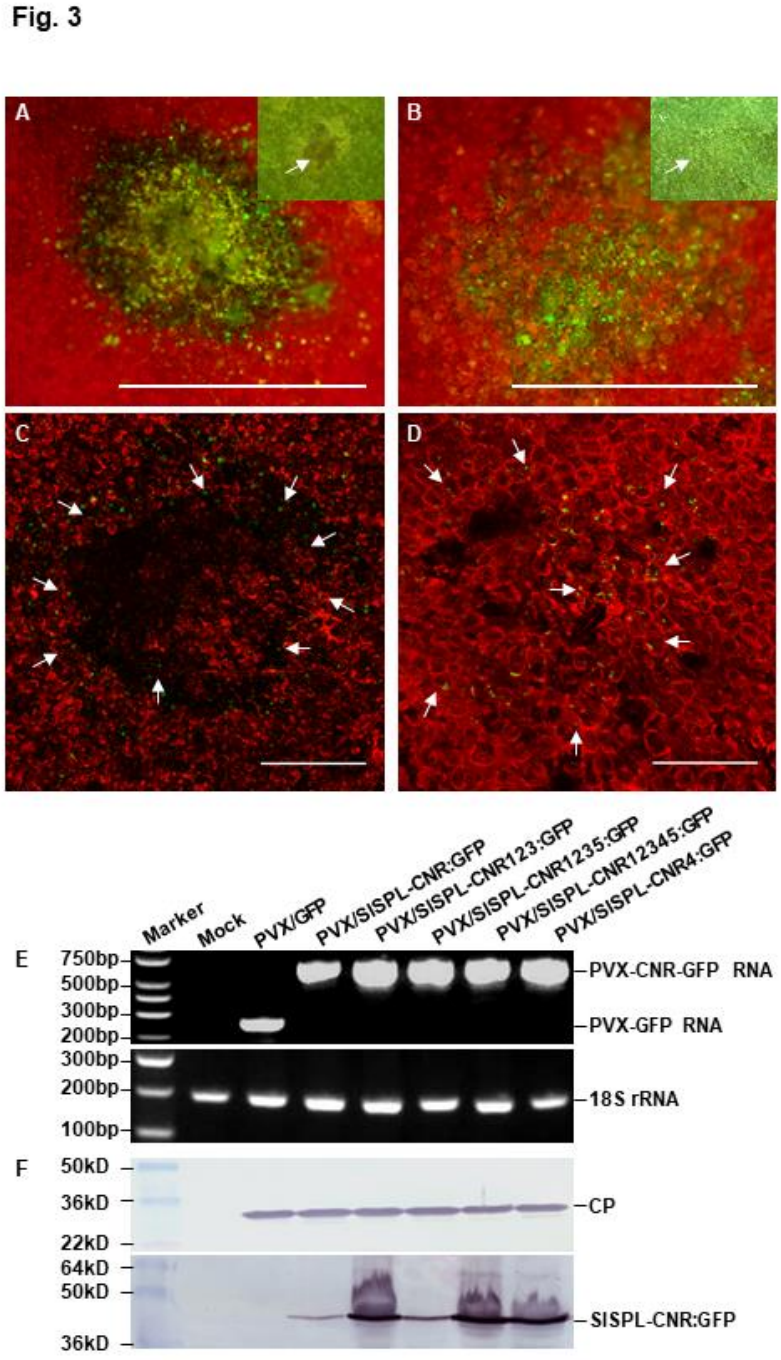

Figure 4

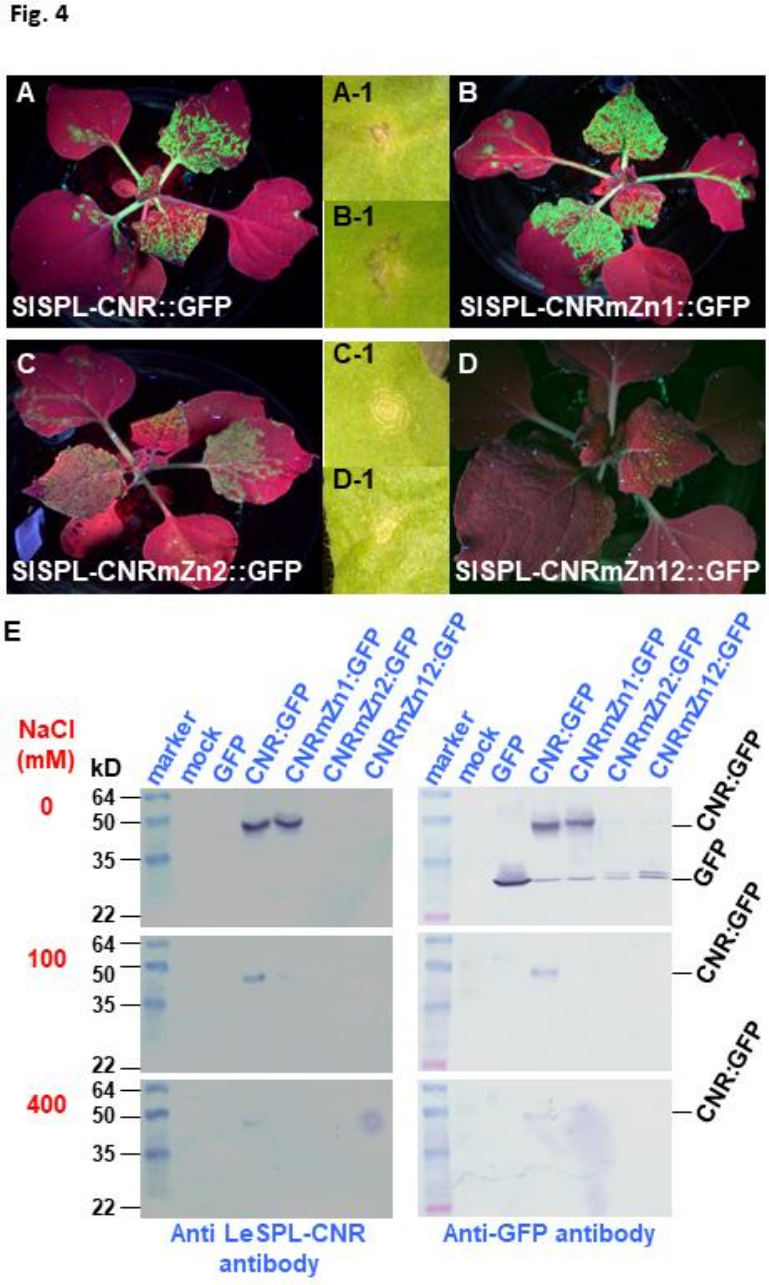

Figure 5

Fig. 5

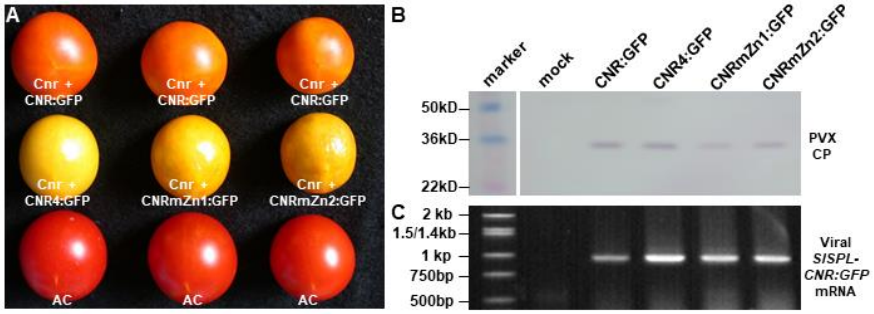

Figure 6

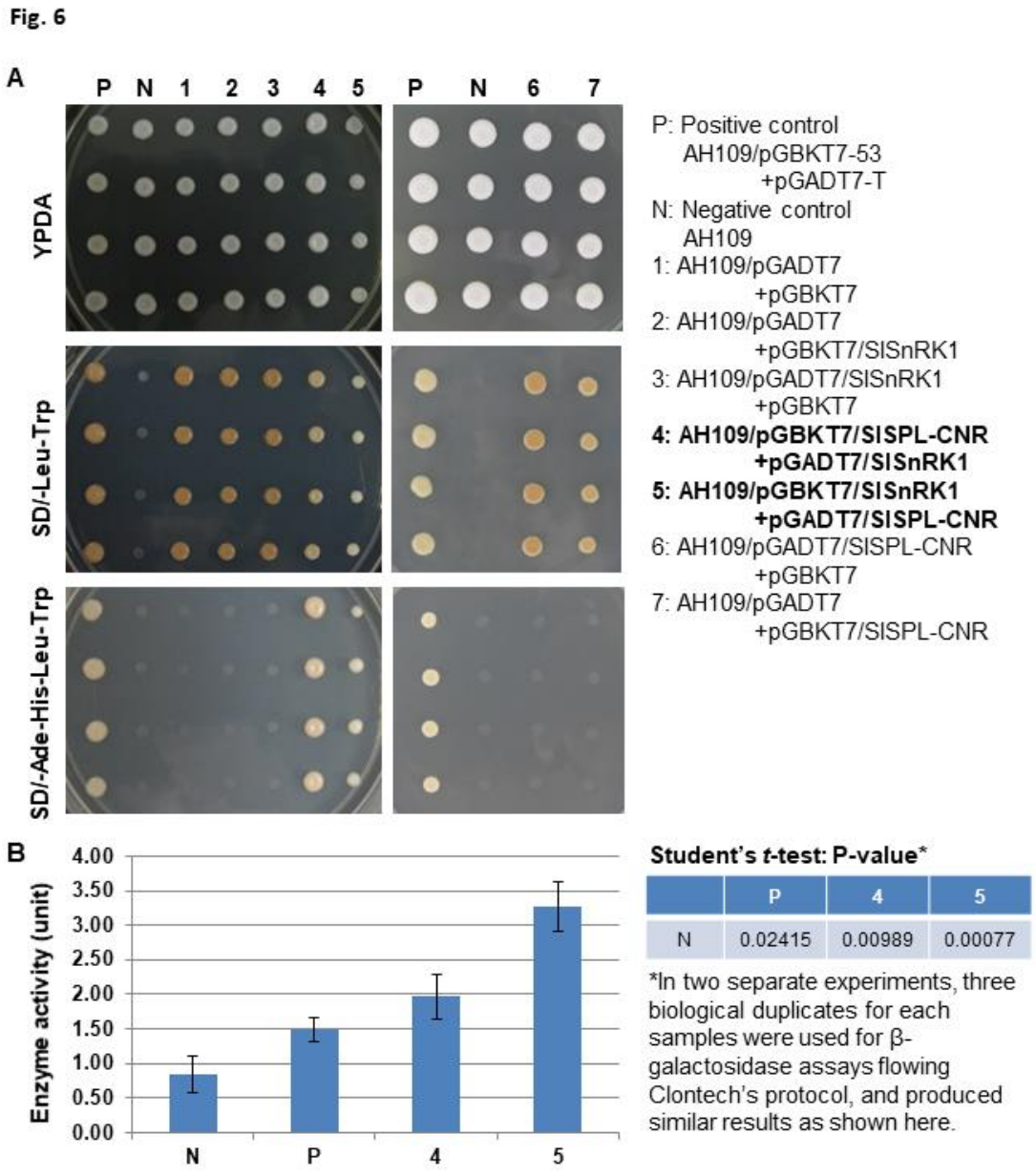

Student's *t*-test: P-value*

	P	4	5
N	0.02415	0.00989	0.00077

*In two separate experiments, three biological duplicates for each samples were used for β-galactosidase assays flowing Clontech's protocol, and produced similar results as shown here.

Figure 7

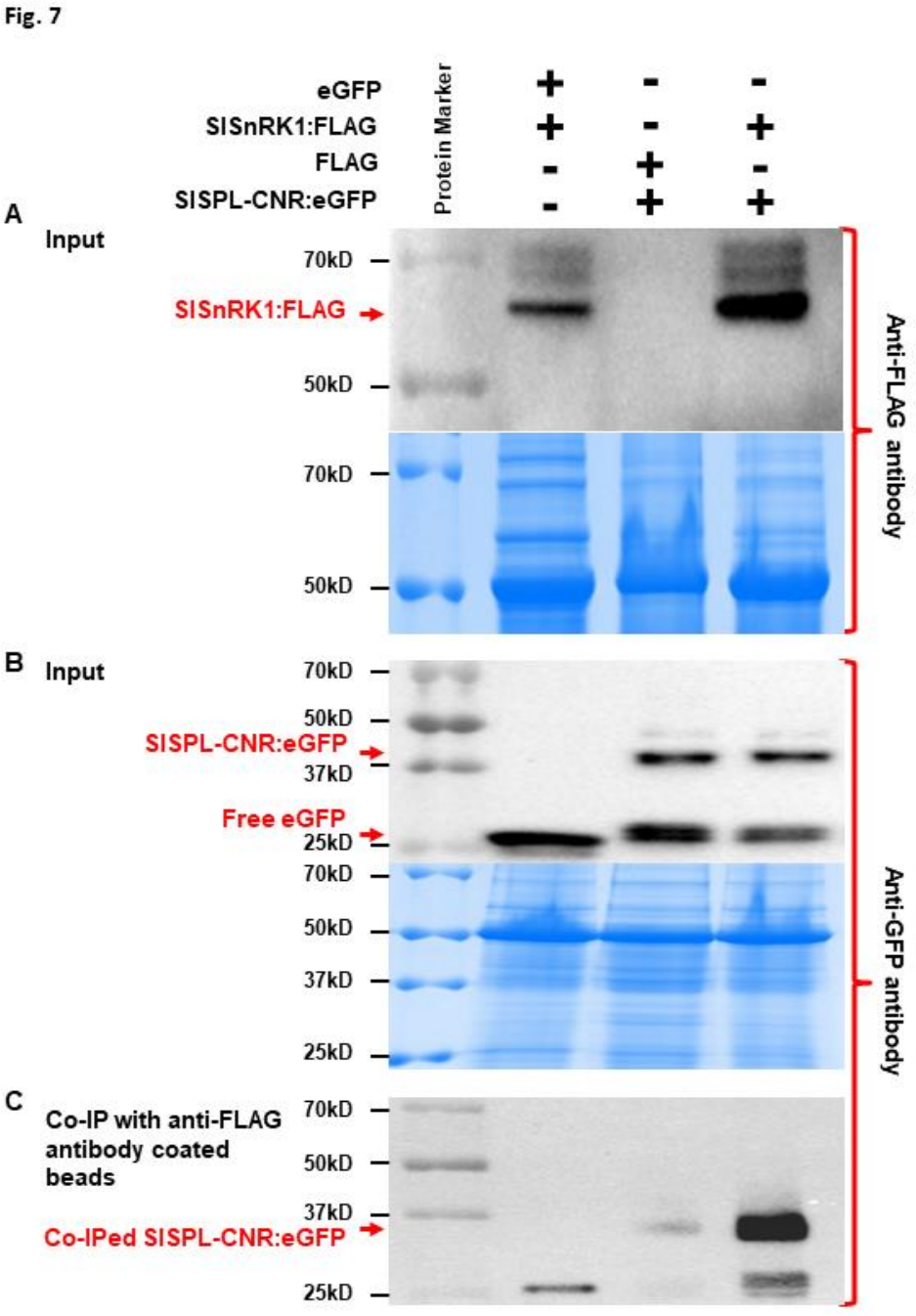

Figure 8

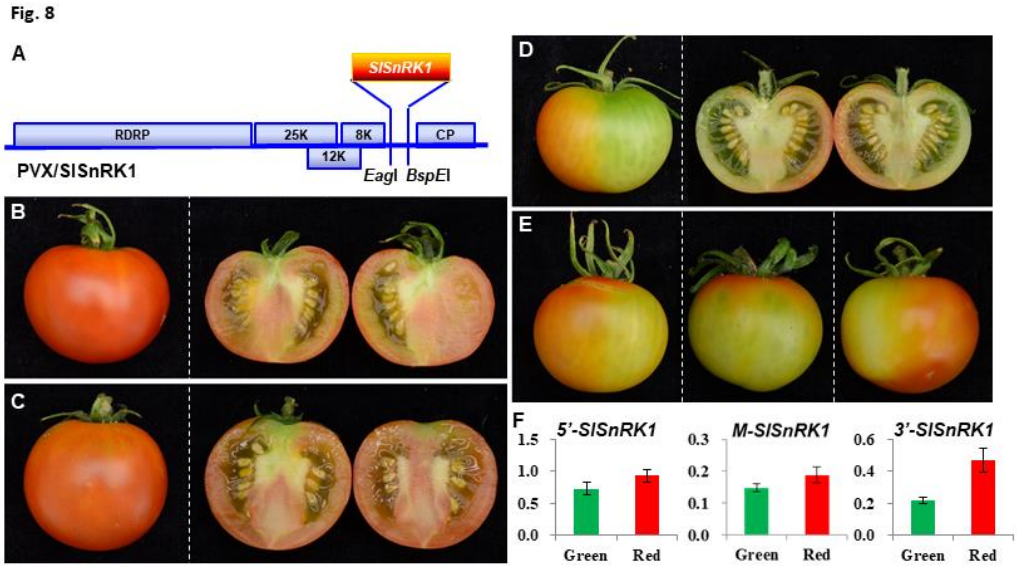

Figure 9